Florida Straits deglacial temperature and salinity change: Implications for tropical hydrologic cycle variability during the Younger Dryas

Matthew W. Schmidt[1] and Jean Lynch-Stieglitz[2]

Received 22 April 2011; revised 19 July 2011; accepted 20 July 2011; published 18 October 2011.

[1] The prevailing paradigm of abrupt climate change holds that rapid shifts associated with the most extreme climate swings of the last glacial cycle were forced by changes in the strength and northward extension of Atlantic Meridional Overturning Circulation (AMOC), resulting in an abrupt reorganization of atmospheric circulation patterns with global teleconnections. To determine the timing of tropical Atlantic atmospheric circulation changes over the past 21 ka BP, we reconstruct high resolution sea surface temperature and $\delta^{18}O_{SW}$ (a proxy for surface salinity) records based on Mg/Ca ratios and oxygen isotope measurements in the planktonic foraminifera *Globigerinoides ruber* from a sediment core located on the western margin of the Florida Straits. As a proxy for meltwater discharge influence on Florida Straits surface water salinity, we also measured Ba/Ca ratios in *G. ruber* from the same core. Results show that riverine influence on Florida Straits surface water started by 17.2 ka BP and ended by 13.6 ka BP, 600 years before the start of the Younger Dryas (YD) cold interval. The initiation of the YD is marked by an abrupt increase in Florida Straits $\delta^{18}O_{SW}$ values, indicating a shift to elevated sea surface salinity occurring in 130 years, most likely resulting from increased regional aridity and/or reduced precipitation. In order to resolve the timing of tropical atmospheric circulation change relative to AMOC variability across this transition, we compare the timing of surface water changes to a recently published record of Florida Current variability in the same core reconstructed from benthic oxygen isotope measurements. We find synchronous changes in atmospheric and ocean circulation on the transition into the YD, consistent with an abrupt reduction in AMOC as the driver of tropical Atlantic atmospheric circulation change at this time.

Citation: Schmidt, M. W., and J. Lynch-Stieglitz (2011), Florida Straits deglacial temperature and salinity change: Implications for tropical hydrologic cycle variability during the Younger Dryas, *Paleoceanography*, *26*, PA4205, doi:10.1029/2011PA002157.

1. Introduction

[2] The last glacial termination was marked by several abrupt climate events, including the Younger Dryas (YD) cold interval that lasted from 12.9–11.7 ka BP. It is generally believed that this last return to glacial conditions in the North Atlantic was caused by a dramatic reduction in North Atlantic Meridional Overturning Circulation (AMOC) triggered by a catastrophic release of freshwater stored in proglacial Lake Agassiz to the northern Atlantic [*Broecker et al.*, 1989; *Kennett and Shackleton*, 1975] or into the Arctic Ocean [*Murton et al.*, 2010], or from the release of freshwater from exceptionally thick sea ice in the Arctic Ocean [*Bradley and England*, 2008]. Regardless of the source of the freshwater, the prevailing paradigm holds that this rapid and extreme climate shift was forced by a reduction in the strength and northward extension of AMOC through its regulation of poleward heat flux [*Alley and Clark*, 1999; *Boyle*, 2000; *Rahmstorf*, 2002], resulting in a synchronous reorganization of global atmospheric circulation patterns, including the weakening of the Asian monsoon system [*Wang et al.*, 2001] and a shift to drier conditions in the tropical North Atlantic [*Haug et al.*, 2001; *Haug et al.*, 2003; *Hughen et al.*, 1998; *Peterson et al.*, 2000; *Peterson and Haug*, 2006].

[3] Coupled ocean-atmosphere general circulation model (GCM) simulations show that a freshwater-induced collapse of AMOC causes an atmospheric circulation response that alters the tropical/subtropical hydrologic cycle by shifting the mean annual position of the Intertropical Convergence Zone (ITCZ) and the North Atlantic Hadley circulation southward [*Dahl et al.*, 2005; *Lohmann*, 2003; *Stouffer et al.*, 2006; *Vellinga and Wood*, 2002; *Zhang and Delworth*, 2005]. As a result, water vapor removal from the North Atlantic is enhanced as freshwater input into the South Atlantic increases. In some GCM simulations, this atmospheric

[1]Department of Oceanography, Texas A&M University, College Station, Texas, USA.
[2]School of Earth and Atmospheric Sciences, Georgia Institute of Technology, Atlanta, Georgia, USA.

0883-8305/11/2011PA002157

feedback mechanism is responsible for an increase in North Atlantic salinity that then stabilizes AMOC [*Krebs and Timmermann*, 2007a, 2007b; *Lohmann and Lorenz*, 2000; *Lohmann*, 2003; *Stouffer et al.*, 2006; *Vellinga and Wu*, 2004]. Accordingly, sea surface salinity (SSS) is predicted to have gradually increased in the tropical/subtropical North Atlantic during periods of reduced AMOC as a result of reduced salt export via North Atlantic Deep Water and/or enhanced hydrologic cycle removal of freshwater out of the North Atlantic basin. According to this 'salt-oscillator hypothesis,' salinity would have gradually increased in North Atlantic surface and upper thermocline waters, eventually reaching a threshold that would force AMOC to restart and shift the climate system into a mild interstadial mode [*Broecker et al.*, 1990; *Lohmann and Lorenz*, 2000; *Lohmann*, 2003; *Zaucker and Broecker*, 1992]. Export of salt from the North Atlantic via AMOC would then gradually reduce North Atlantic salinity and precondition the system for a return to stadial conditions.

[4] Several proxy reconstructions of tropical Atlantic salinity variation over the last glacial cycle are consistent with an increase in low-latitude SSS during high-latitude cold periods. *Schmidt et al.* [2004] and *Schmidt and Spero* [2011] combined Mg/Ca-sea surface temperature (SST) with $\delta^{18}O_{CALCITE}$ ($\delta^{18}O_C$) measurements on the surface-dwelling foraminifera *Globigerinoides ruber* (white variety) from western Caribbean sediment cores to reconstruct past variation in tropical Atlantic $\delta^{18}O_{SEAWATER}$ ($\delta^{18}O_{SW}$) (a proxy for sea surface salinity (SSS)) over several of the last glacial periods. Their results demonstrated that Caribbean $\delta^{18}O_{SW}$ is highly variable and linked to inferred changes in AMOC. In particular, enrichments in $\delta^{18}O_{SW}$ occurred during glacial intervals and then return to modern or more negative values during interglacials. Using the same methodology, *Weldeab et al.* [2006] found parallel $\delta^{18}O_{SW}$ enrichments in the western tropical Atlantic during cold phases of the last deglacial and *Carlson et al.* [2008] showed that cold-phase $\delta^{18}O_{SW}$ enrichments extended into both the northern and southern subtropical gyres of the Atlantic. $\delta^{18}O_{SW}$ enrichments were also calculated for the North Atlantic subtropical gyre during the cold Dansgaard-Oeschger stadial events of Marine Isotope Stage (MIS) 3 [*Schmidt et al.*, 2006] and in the Florida Current during the Little Ice Age [*Lund and Curry*, 2006]. These researchers conclude that North Atlantic SSS enrichments during cold phases in the North Atlantic resulted from a combination of 1) changes in the tropical/subtropical hydrologic cycle and/or 2) large-scale changes in ocean circulation resulting in reduced heat and salt transport to the North Atlantic. However, age model uncertainties and resolution limitations in these studies make it difficult to determine the phasing between low-latitude hydrologic system change relative to AMOC variability across abrupt climate events.

[5] Here, we reconstruct tropical SST and SSS change over the last 21 ka BP using combined Mg/Ca-paleothermometry and stable oxygen isotope measurements in the planktonic foraminifera *Globigerinoides ruber* (white variety) from a high-sedimentation rate core located on the western margin of the Florida Straits. Because riverine water has a much higher concentration of dissolved barium ($[Ba^{2+}]$) [*Weldeab et al.*, 2007], we also measured Ba/Ca ratios in *G. ruber* tests as a proxy for the influence of deglacial meltwater on the salinity of Florida Straits surface water across the deglacial. In order to resolve the phasing between atmospheric versus ocean circulation changes across the YD cold interval, we then compare the timing of surface water hydrographic variability to the recently published record of oxygen isotope change in benthic foraminifera (a proxy for Florida Current transport) in the same core [*Lynch-Stieglitz et al.*, 2011].

2. Oceanographic Setting

[6] For this study, we used a high-sedimentation rate core recovered from the western margin of the Florida Straits near the Dry Tortugas, KNR166-2-26JPC (24°19.61′N, 83°15.14′W; 546 m depth) (Figure 1). Waters from the Caribbean and the tropical Atlantic are directly connected with waters on the eastern margin of the Florida Straits via flow through the Yucatan Current [*Murphy et al.*, 1999; *Schmitz and Richardson*, 1991]. As such, waters on the western margin of the Florida Straits are predominantly characteristic of the Caribbean and form an important link between waters of the Caribbean, the Gulf of Mexico and North Atlantic.

[7] The modern seasonal SST cycle in the Florida Straits varies from a low of 25 to 26°C (0 m depth) from December through March and then increases to a maximum of 29.0 to 29.4°C from July to mid-September [*Locarnini et al.*, 2006]. The modern average annual SST is 27.5°C [*Locarnini et al.*, 2006]. Mesoscale cyclonic eddies form near the Dry Torguas during periods of strong Loop Current development [*Fratantoni et al.*, 1998]. These frontal eddies associated with the Loop Current can persist for about 100 days and their presence acts to cool SSTs during winter and spring when surface temperatures in the Gulf of Mexico are cooler than in the Florida Current [*Fratantoni et al.*, 1998].

[8] In the modern tropical Atlantic and Caribbean region, annual salinity variability is primarily controlled by the seasonal migration of the ITCZ between 15°N and 5°S [*Waliser and Gautier*, 1993]. Evaporation/precipitation (E/P) ratios decrease during the boreal summer months when the ITCZ is located farthest to the north and then increase during the cool, dry season as the ITCZ migrates southward during boreal winter [*Stidd*, 1967]. Modern annual SSS varies from a high of 36.1 to 36.2 from January to June and decreases to a low of ~35.9 from August to December [*Antonov et al.*, 2010]. Modern annual SSS (0 m depth) near the Dry Tortugas averages ~36.1 [*Antonov et al.*, 2010].

3. Materials and Methods

3.1. Age Model Development

[9] As previously discussed in *Lynch-Stieglitz et al.* [2011], out of sequence radiocarbon dates were found in a section of 26JPC from 344–408 cm. Closer examination of the core revealed layers of coarse material from 352–418 cm [see *Lynch-Stieglitz et al.*, 2011, Figure 3]. The coarse layers do not show evidence for turbidite deposition and often do not extend across the entire core. Instead, the coarse layers resemble contourite deposits like those found in the deep western boundary current, indicative of high bottom current speeds. It is possible that discrete layers in this section of the core experienced lateral transport of older sediments and we therefore consider this entire section of the core as poten-

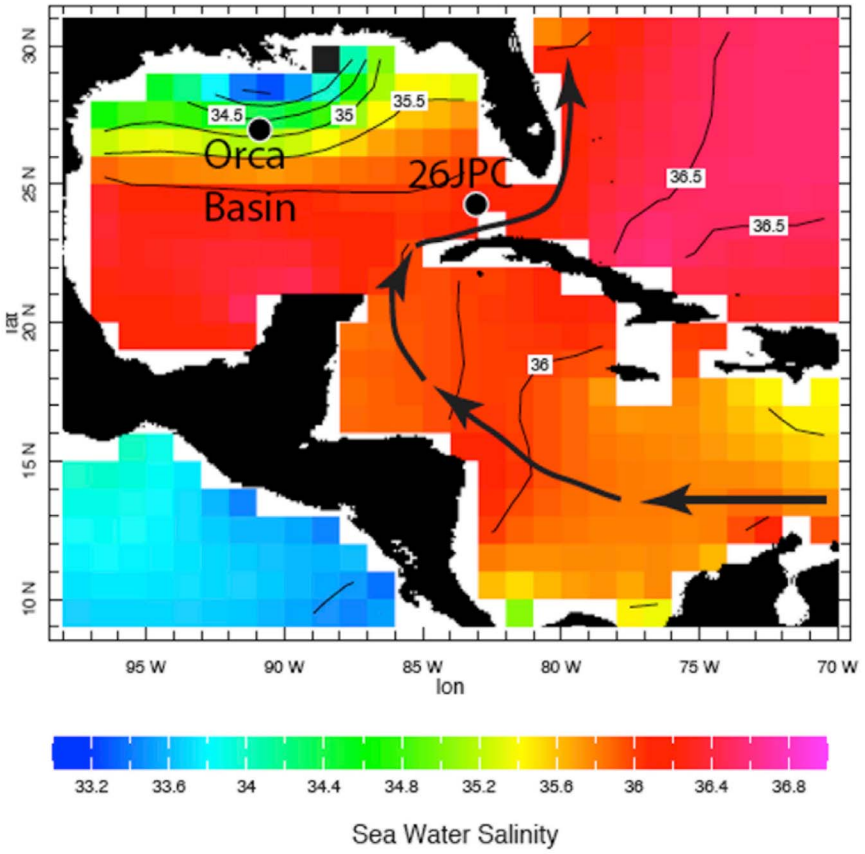

Figure 1. Mean annual sea surface salinity in the northern Caribbean, Florida Straits and Gulf of Mexico [*Antonov et al.*, 2010]. The location of KNR166-2-26JPC on the western margin of the Florida Straits and the Orca Basin in the northern Gulf of Mexico are indicated with black circles. Surface current flow through the Caribbean and the Florida Straits is shown with the black arrows. Salinity in the Florida Current is dominated by the advection of low salinity surface waters from the Caribbean and tropical North Atlantic.

tially disturbed (gray bar on Figure 2). However, no other sections of the core contained coarse layer deposits or out of sequence radiocarbon dates, so it is likely that any lateral sediment transport was confined to this one section of 26JPC. Radiocarbon dates from this section of the core were not used in the age model.

[10] The age model for 26JPC was developed using previously published accelerator mass spectrometry ^{14}C dates given by *Lynch-Stieglitz et al.* [2011] (Table 1). The ^{14}C ages were converted to calendar age using Calib 6.0 (M. Stuiver et al., Calib calibration program, version 6.0, 2011) using the standard marine reservoir correction [*Hughen et al.*, 2004] (Figure 2d) and assuming linear sedimentation rates between the age control points. The resulting age model indicates highest sedimentation rates of 170 cm/ka from 13–11 ka BP and lower sedimentation rates of 30 cm/ka from 21–13 ka BP. The disturbed interval occurs during a period of extremely high sedimentation rates between 344 and 418 cm and corresponds to a 450-year period between 11.50–11.95 ka BP, noted by a gray bar on Figure 2. However, it is important to note that the transition into the YD at 12.9–13.0 ka BP and the first 500 years of the YD does not fall within the disturbed section of the core.

3.2. Isotopic Analysis

[11] The planktonic and benthic stable oxygen isotope data presented in this paper were previously published by *Lynch-Stieglitz et al.* [2011]. In summary, sediment from each 2 cm interval was disaggregated in deionized water, sieved and dried at room temperature. To minimize ontogenetic and growth rate effects on shell geochemistry, specimens of *G. ruber* (white variety) were only collected from the 250–350 μm size fraction [*Lea et al.*, 2000] and the benthic foraminifera *Cibicidoides pachyderma* were collected from the >250 μm size fraction. All samples were first sonicated in methanol for 3–8 s and oxygen isotope values were then measured using a GV Instruments Isoprime mass spectrometer with Multiprep (Georgia Tech), Finnigan MAT 253 mass spectrometer with Kiel Device (WHOI and Georgia Tech), and GV Instruments Optima with Multiprep (LDEO) and calibrated with NBS-19 and NBS-18. *G. ruber* oxygen isotope values are based on 10–12 individuals per interval and 31% of the intervals were run in duplicate. The average standard deviation on intervals with at least two $\delta^{18}O$ analyses based on 12 individuals each is 0.18‰. Natural $\delta^{18}O$ variability within a population will result in a larger standard deviation when two groups of 12 individuals are

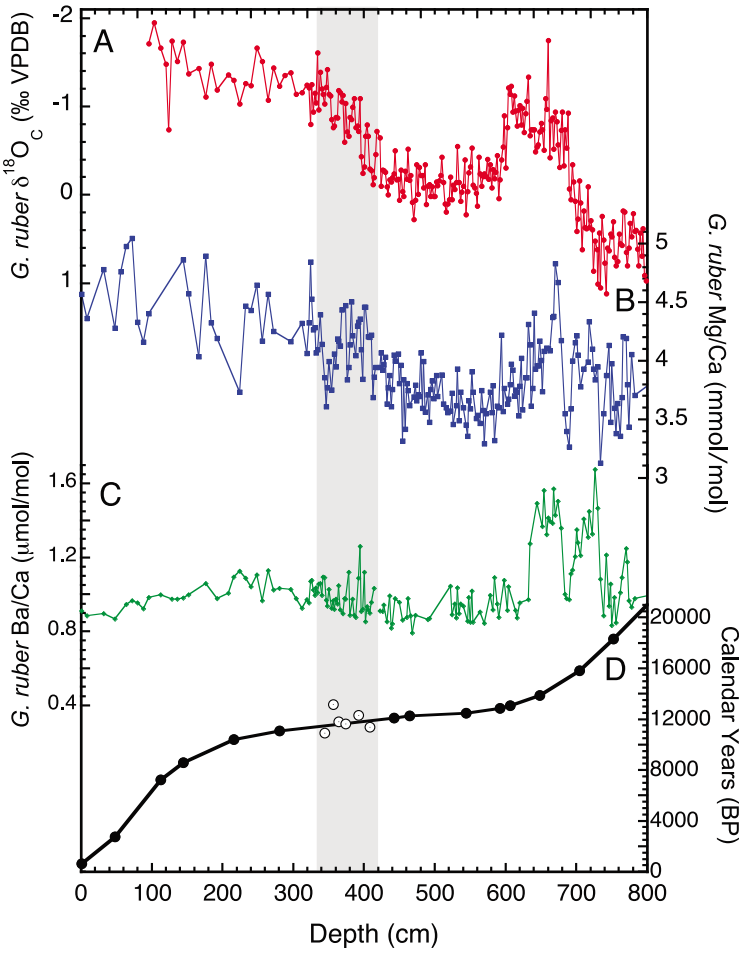

Figure 2. (a) Oxygen isotope values in the planktonic foraminifera *G. ruber* (white) from 26JPC, previously published by *Lynch-Stieglitz et al.* [2011]. (b) Mg/Ca ratios and (c) Ba/Ca ratios in *G. ruber* (white) from the same core plotted versus depth. (d) Age model for 26JPC, based on radiocarbon ages plotted with solid black circles. The radiocarbon ages with open circles located between 344 and 408 cm were not used in the age model. All radiocarbon ages were converted to calendar ages using Calib 6.0 (M. Stuiver et al., Calib calibration program, version 6.0, 2011) using the standard marine reservoir correction [*Hughen et al.*, 2004]. The gray shaded region notes the interval in the core containing the out of sequence radiocarbon dates and should be interpreted with caution.

analyzed as compared to crushing and homogenizing 24 individuals and running the split twice. Benthic oxygen isotope values are based on groups of 3–5 individuals per interval.

3.3. Trace Metal Analysis

[12] Metal/Ca (Me/Ca) ratios were measured on the same population and size fraction of *G. ruber* specimens used for the stable isotope analyses. Whenever enough sample material was available, ~570 μg of *G. ruber* shell/sample (~45–55 shells) was crushed, homogenized, split and then cleaned for trace element analysis according to the procedures by *Lea and Martin* [1996] and *Mashiotta et al.* [1999] without the DTPA step. In brief, samples underwent a multistep process consisting of initial rinses in ultra-pure water, followed by treatments with hot reducing and oxidizing solutions, transfers into new acid-leached microcentrifuge vials, and finally leaches with a dilute ultra-pure acid solution (0.001 N HNO_3). All clean work was conducted in laminar flow benches under trace metal clean conditions. Samples were then dissolved and analyzed for Me/Ca ratios on a Jobin Yvon ICP-OES at Georgia Tech according to the methods of *Schrag* [1999] or on a Thermo Scientific Element XR High Resolution Inductively Coupled Mass Spectrometer (HR-ICP-MS) at Texas A&M University using isotope dilution, as outlined by *Lea and Martin* [1996] and *Lea et al.* [2000]. The average Mg/Ca ratio of samples analyzed by both methods varied by less than 2.5%. A suite of elements including Na, Mg, Ca, Sr, Ba, U, Al, Fe and Mn, were analyzed and reported as Me/Ca ratios. Analyses with anomalously high (>100 μmol/mol) Al/Ca, Fe/Ca or Mn/Ca ratios or with low percent recovery (<20%) were rejected. Analyses with high Al/Ca indicate the presence of detrital clays that were not removed during the cleaning process. Elevated levels of Fe/Ca or Mn/Ca indicate the presence of diagenetic coatings that were not removed during the cleaning process. Low percent recovery values indicate the loss of shell material during the cleaning

Table 1. Twenty-Six JPC Radiocarbon Dates[a]

Depth (cm)	Species	^{14}C Age	Error	Calendar Age	Error (±yr)
0.75	*G. sacculifer*	1070	70	635	118
48.25	*G. sacculifer*	2990	30	2772	66
112.25	*G. sacculifer*	6720	40	7250	95
144.25	*G. sacculifer*	8100	80	8613	229
216.25	*G. sacculifer*	9550	40	10398	121
280.25	*G. sacculifer*, *G. ruber*	10100	45	11115	94
344.25	*G. sacculifer*	10000	110	10913[b]	275
356.25	*G. sacculifer*	11750	95	13190[b]	217
364.25	*G. sacculifer*, *G. ruber*	10600	70	11795[b]	384
374.25	*G. sacculifer*	10500	50	11643[b]	268
392.25	*G. ruber*	10850	65	12337[b]	236
408.25	*G. sacculifer*, *G. ruber*	10300	60	11392[b]	229
442.25	*G. sacculifer*, *G. ruber*	10700	65	12095	251
464.25	*G. sacculifer*, *G. ruber*	10800	55	12278	249
544.25	*G. sacculifer*, *G. ruber*	11000	65	12505	154
592.25	*G. ruber*	11400	65	12880	199
606.25	*G. sacculifer*	11600	35	13064	156
648.25	*G. sacculifer*	12350	200	13885	583
704.25	*G. ruber*	13500	55	15834	615
752.25	*G. ruber*	15550	70	18326	297
848.25	*G. ruber*	20300	120	23776	419

[a]Calibrated using Calib 6.0 and Marine09 curve with a 400 year surface reservoir age.
[b]Not used in age model.

process, most likely due to human error. All trace metal and oxygen isotope data will be archived at the World Data Center-A for Paleoclimatology located in Boulder, Colorado at the U.S. National Oceanic and Atmospheric Administration (NOAA) National Climatic Data Center (NCDC) Paleoclimatology Program.

3.4. Calculations

[13] Mg/Ca ratios were converted to SST using the all-species planktonic relationship of *Anand et al.* [2003]:

$$\mathrm{Mg/Ca} = 0.38\ \exp(0.09{*}\mathrm{T}) \quad (1)$$

This equation (1) was derived from the calibration of Mg/Ca ratios to SST in 10 species of planktonic foraminifera collected from sediment traps in the Sargasso Sea. Given the shallow depth of 26JPC (542 m), we chose to use this equation because it does not have dissolution biases inherent in core top calibrations developed from deeper sites. To compute $\delta^{18}O_{SW}$, the Mg/Ca-based SST is removed from the $\delta^{18}O_C$ record using the following temperature: $\delta^{18}O$ relationship from *Bemis et al.* [1998]:

$$\mathrm{SST}(^\circ\mathrm{C}) = 16.5 - 4.80\left(\delta^{18}O_C - \left(\delta^{18}O_{SW} - 0.27‰\right)\right) \quad (2)$$

Lea et al. [2000] and *Schmidt et al.* [2004] found that this relationship determined for *Orbulina universa* in laboratory culture experiments [*Bemis et al.*, 1998] yields excellent results when applied to fossil *G. ruber* (white variety) to calculate modern $\delta^{18}O_{SW}$ in the equatorial Pacific and Caribbean.

[14] On glacial time scales, $\delta^{18}O_{SW}$ is also affected by variations in continental ice volume because the formation of continental ice sheets preferentially removes $H_2^{16}O$ from the ocean. In order to remove the continental ice volume contribution from the Florida Straits $\delta^{18}O_{SW}$ record, we generated a high-resolution record of global $\delta^{18}O_{SW}$ change over the last glacial termination using the sea level data by *Siddall et al.* [2009] and assume the 120 m Last Glacial Maximum (LGM) sea level drop corresponds to a 1.05‰ change in global seawater $\delta^{18}O_{SW}$ change [*Schrag et al.*, 2002]. Removal of global $\delta^{18}O_{SW}$ change resulting from the melting of continental ice sheets results in the record of regional ice volume free-$\delta^{18}O_{SW}$ (IVF-$\delta^{18}O_{SW}$) change, allowing for the evaluation of high-resolution regional surface water $\delta^{18}O$ variability.

3.5. Error Analysis

[15] Long-term analytical precision for the $\delta^{18}O_C$ measurements is better than ±0.08‰. The long-term analytical reproducibility of a synthetic, matrix-matched Mg/Ca standard analyzed by ICP-OES based on a synthetic standard with a matched foraminiferal Mg/Ca concentration is 0.65%, and the long-term analytical reproducibility of a synthetic, matrix-matched Mg/Ca standard analyzed by HR-ICP-MS over the course of this study is ±0.48%. The pooled standard deviation of all replicate Mg/Ca analyses measured by both methods is ±3.8% (1 SD, degrees of freedom = 164) based on 214 analyzed intervals. Given the average Mg/Ca ratio of 3.96 mmol/mol for samples from this study, this equates to an error of ±0.15 mmol/mol, or ±0.41°C using equation (1).

[16] In order to estimate the error on our calculated $\delta^{18}O_{SW}$ values, we propagate the 1σ analytical error on our $\delta^{18}O_C$ values and the pooled standard deviation value of our Mg/Ca replicates with the reported error on calibration equations (1) and (2), resulting in an error of ±0.25‰. Using a variety of methods, previous studies report similar error propagations for the $\delta^{18}O_{SW}$ residuals based on $\delta^{18}O_C$ and Mg/Ca-SSTs in *G. ruber*, ranging from ±0.18‰ to ±0.26‰ [*Carlson et al.*, 2008; *Lea et al.*, 2000; *Lund and Curry*, 2006; *Oppo et al.*, 2009; *Schmidt et al.*, 2004, 2006; *Weldeab et al.*, 2006].

[17] The long-term analytical reproducibility of our synthetic Ba/Ca standard is ±0.50%. The pooled standard deviation on replicate Ba/Ca analyses from 26JPC is ±5.07% (1 SD, degrees of freedom = 45) based on 165 analyzed intervals. The average Ba/Ca ratio in the record is 1.03 μmol/mol so the analytical error for the reported Ba/Ca ratios is ±0.05 μmol/mol.

4. Results and Discussion

4.1. Deglacial Sea Surface Temperature Reconstruction

[18] Using equation (1), the calculated core top SST for 26JPC is 27.6°C (core top age = 635 years). The modern seasonal SST cycle in the Florida Straits varies from ~25.5 to 29.4°C (0 m depth) with a modern average annual SST of 27.5°C [*Locarnini et al.*, 2006]. Therefore, the calculated core top temperature is well within the ±1°C calibration uncertainty [*Anand et al.*, 2003].

[19] The 26JPC deglacial temperature record calculated from equation (1) indicates minimum SSTs of ~24.0°C during parts of the early YD and from 18.9 to 17.4 ka BP (Figure 3b), resulting in a maximum cooling of ~3.0°C during the YD and the early deglaical relative to the modern. Combining the analytical uncertainty on the Mg/Ca measurements (±0.41°C) with the Mg/Ca:SST calibration error

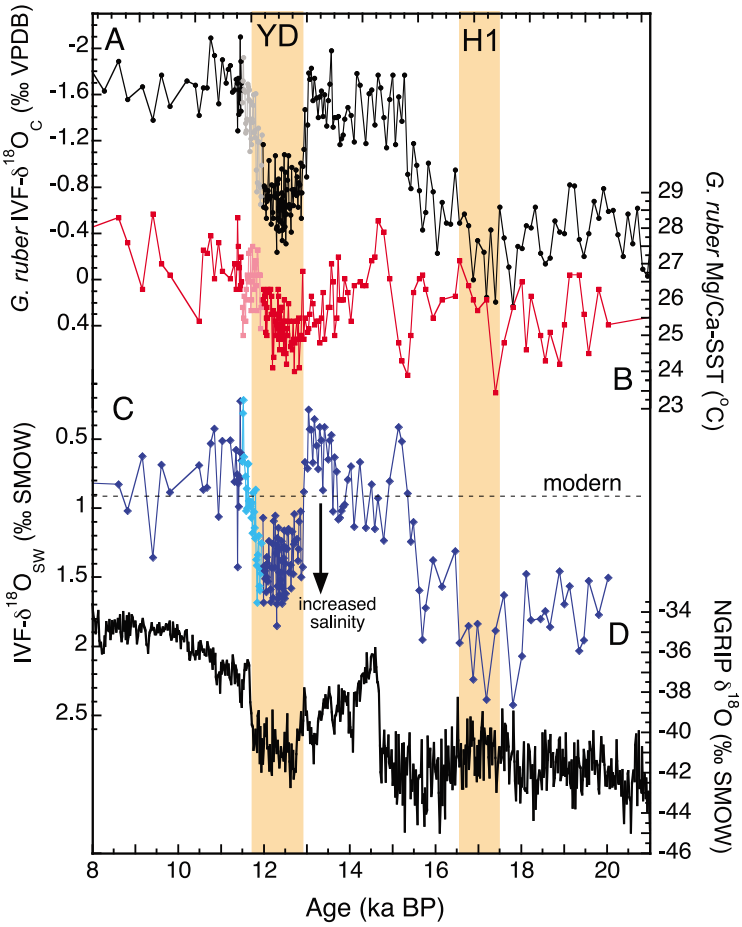

Figure 3. (a) Ice volume free (IVF) *G. ruber* $\delta^{18}O_C$ values from 26JPC plotted versus age from 8 to 21 ka BP. The oxygen isotope values have been corrected for whole ocean $\delta^{18}O_{SW}$ change due to the melting of continental ice sheets using the sea level data in *Siddall et al.* [2009]. (b) Mg/Ca-SSTs in 26JPC converted to SST using equation (1) [*Anand et al.*, 2003]. (c) Computed IVF-$\delta^{18}O_{SW}$ calculated from the Mg/Ca-derived SST and $\delta^{18}O_C$ using equation (2) [*Bemis et al.*, 1998]. The dashed horizontal line indicates the modern local $\delta^{18}O_{SW}$ value. Note the reverse axis with positive down. (d) Oxygen isotopes in the NGRIP ice core showing the timing of colder conditions (low $\delta^{18}O$) in Greenland [*Andersen et al.*, 2004; *Rasmussen et al.*, 2006]. Shaded regions indicate the Younger Dryas (YD) and Heinrich Event 1 (H1), and the data plotted in lighter shades are from the interval in the core with the out of sequence radiocarbon ages.

(±1°C), this amount of cooling during the YD and early deglacial exceeds our estimated combined error. The 26JPC SST record also indicates a warm interval from 17.2 to 15.4 ka BP when average SSTs were ~26.2°C. Temperatures then decreased to 24°C at 15.3 ka BP before rapidly increasing to near modern temperatures at the start of the Bølling-Allerød (BA) at 14.7 ka BP. The transition into the YD is not associated with an abrupt cooling. Instead, SSTs gradually decrease after the brief BA warm interval, reaching minimum values near 24°C by the start of the YD at 13.0 ka BP. Temperatures then remain cool from 12.9 to 12.2 ka BP, averaging 25.1°C. The 26JPC SST record suggests that temperatures began to warm in the Florida Straits sometime around 12.1 ka BP and reached near-modern values by 11.8 ka BP; however, these dates are within the section of the core with the out of sequence ^{14}C dates, so the timing of temperature change on this transition should be viewed with caution.

[20] Previous modeling studies have shown that a cooling in the North Atlantic associated with a weakening of AMOC is transmitted to the tropical Atlantic through both atmospheric [*Chiang et al.*, 2008] and oceanic processes [*Chang et al.*, 2008]. In an effort to isolate the impact of these changes on western tropical Atlantic SST, *Wan et al.* [2009] used a set of GCM experiments to show that atmospheric circulation changes result in a minor surface cooling (1–2°C) while ocean circulation changes result in a larger, subsurface warming in the tropical Atlantic. *Wan et al.* [2009] showed that locations influenced by local upwelling could have experienced a surface warming during periods of reduced AMOC. Therefore, it is not surprising that some proxy-based SST reconstructions from the western tropical Atlantic indicate a warming during the YD [*Hüls and Zahn*, 2000; *Rühlemann et al.*, 1999] and others a significant cooling [*Lea et al.*, 2003; *Guilderson et al.*, 2001]. Although *Lea et al.* [2003] calculated a 4°C cooling in the Cariaco Basin at the

start of the YD, *Wan et al.* [2009] showed that this magnitude of cooling was not consistent with most GCM hosing experiments and instead reflects a local dynamic response restricted to inside the Cariaco Basin rather than being representative of the open Caribbean.

[21] Today, water flows more directly from the Yucatan Channel into the Florida Straits during periods of reduced Loop Current penetration [*Lee et al.*, 1995]. Periods of reduced Loop Current penetration also result in the formation of fewer Tortugas eddies [*Lee et al.*, 1995]. This results in a shift in the axis of the Florida Current northward and warmer SSTs at our study site due to an increase in the component of warm Caribbean surface water. Although instrumental data suggests that eddy formation today is stochastic and unrelated to climate forcing [*Maul and Vukovich*, 1993; *Vukovich*, 1988; *Sturges and Leben*, 2000], a reduction in the penetration of the Loop Current into the Gulf of Mexico during past climate events could have resulted in a slight warming in our record. *Nürnberg et al.* [2008] showed that Loop Current influence on SSTs in the northeastern Gulf of Mexico diminished during glacial periods, suggesting a weakening of the Loop Current during cold phases in the North Atlantic. If Loop Current penetration and Tortugas eddy formation was dramatically reduced during the YD and H1, atmospheric cooling at our study site may have been moderated by a slight warming caused by the presence of more warm Caribbean surface water near the Dry Tortugas at these times. This may explain the relatively small amount of SST cooling observed in our record during the YD and for most of the early deglacial.

4.2. Deglacial $\delta^{18}O_{SW}$ and Sea Surface Salinity

[22] By combining the *G. ruber* Mg/Ca-SST values with paired $\delta^{18}O$ analyses, we calculate $\delta^{18}O_{SW}$ change across the deglacial using equation (2). Correcting for global $\delta^{18}O_{SW}$ change due to continental ice volume variation [*Siddall et al.*, 2009] results in the record of local IVF-$\delta^{18}O_{SW}$ (Figure 3c). Because $\delta^{18}O_{SW}$ covaries linearly with SSS [*Charles and Fairbanks*, 1990], reconstructed IVF-$\delta^{18}O_{SW}$ values can be used to estimate past SSS change. Most of the waters on the western margin of the Florida Straits originate in the Caribbean and tropical Atlantic [*Schmitz and Richardson*, 1991], so we can use the modern $\delta^{18}O_{SW}$:SSS relationship for the open Caribbean ($\delta^{18}O_{SW}$ ‰ = 0.26 * SSS − 8.44) [*Schmidt et al.*, 1999] to estimate a modern $\delta^{18}O_{SW}$ value based on the modern annual salinity. *Lund and Curry* [2006] used this same approach when reconstructing late Holocene SSS and $\delta^{18}O_{SW}$ variability in another Florida Margin core located near our study site. Given the modern average SSS at our study site of 36.1 [*Antonov et al.*, 2010], the modern local $\delta^{18}O_{SW}$ value is estimated to be 0.95‰. This is in good agreement with the average Holocene IVF-$\delta^{18}O_{SW}$ value of 0.90‰ (9.8–6.1 ka BP) calculated for 26JPC.

[23] The 26JPC deglacial IVF-$\delta^{18}O_{SW}$ record indicates that $\delta^{18}O_{SW}$ values in the Florida Straits were more positive (saltier) than the modern prior to 15.5 ka BP and again during the YD (Figure 3c). The most positive IVF-$\delta^{18}O_{SW}$ values across the deglacial occur prior to and during Heinrich Event 1 (H1) when values were more than 1.0‰ heavier than modern. The YD was also a time of enriched IVF-$\delta^{18}O_{SW}$ when values averaged 0.43‰ heavier than the modern from 12.9–11.8 ka BP (Figure 3c).

[24] Although most waters flowing through the Florida Straits today originate in the Caribbean and tropical Atlantic, large meltwater discharges into the Gulf of Mexico from the Mississippi River and the southeastern United States most likely impacted $\delta^{18}O_{SW}$ values in the Florida Straits at certain times during the deglacial period, making it difficult to constrain the $\delta^{18}O_{SW}$:SSS relationship at times in the past. This issue was encountered by *Flower et al.* [2004] when they used Mg/Ca-SSTs and $\delta^{18}O_C$ analyses in fossil *G. ruber* specimens from the Orca Basin (northern Gulf of Mexico) to generate a record of $\delta^{18}O_{SW}$ change across the deglacial (Figure 4c). The Orca Basin IVF-$\delta^{18}O_{SW}$ record indicates a period of elevated meltwater discharge into the Gulf of Mexico starting around 16 ka BP and lasting until the start of the YD at around 12.9 ka BP. Because meltwater discharges originating from the Laurentide ice sheet had a much more negative $\delta^{18}O$ value (−25‰ to −35‰ [*Fairbanks*, 1989]) relative to local precipitation (−7‰ [*Ortner et al.*, 1995]), past meltwater inputs would have significantly changed the local $\delta^{18}O_{SW}$:SSS relationship. Therefore, in order to estimate SSS change from our deglacial IVF-$\delta^{18}O_{SW}$ record, we need to determine when glacial meltwater potentially impacted $\delta^{18}O_{SW}$ values in the Florida Straits and when local $\delta^{18}O_{SW}$ values reflect regional E/P ratios.

4.3. Deglacial Ba/Ca Reconstruction

[25] To determine when major meltwater discharges into the Gulf of Mexico influenced $\delta^{18}O_{SW}$ values in the Florida Straits, we measured Ba/Ca ratios in *G. ruber* from 26JPC across the deglacial (Figures 2c and 4b). The desorption of Ba^{2+} from suspended sediments in rivers results in a much higher riverine [Ba^{2+}] relative to seawater. Once the particulate sediments are deposited in river estuaries, the dissolved [Ba^{2+}] exhibit conservative mixing with seawater, resulting in a linear inverse correlation between salinity and [Ba^{2+}] [*Coffey et al.*, 1997; *Edmond et al.*, 1978; *Hanor and Chan*, 1977]. Culturing experiments indicate that Ba^{2+} incorporation into living planktonic foraminifera shells is linear, dependent primarily on the [Ba^{2+}] of the water in which the shell grows [*Hönisch et al.*, 2011; *Lea and Spero*, 1994]. Therefore, Ba/Ca ratios in foraminifera living in a region influenced by a source of high dissolved Ba^{2+} input (such as the Mississippi River) can be used to estimate past SSS changes based on the regional [Ba^{2+}]:SSS relationship [*Hall and Chan*, 2004; *Weldeab et al.*, 2007].

[26] Although the modern Mississippi River discharge is too small to directly impact SSS in the Florida Straits today, it is likely that discharge rates were much higher during major meltwater events of the last deglacial period. Large meltwater discharges would have caused elevated rates of erosion with the potential to supply more river borne clay to local estuaries. During these times, it is possible the riverine [Ba^{2+}] was significantly higher than modern. Therefore, it is not possible to assume the barium flux is proportional to river discharge rates. In fact, *Mitchell et al.* [2001] showed the rate of barium flux in alpine glacier meltwater can significantly increase at elevated discharge rates. Because we do not have data constraining past Gulf of Mexico riverine [Ba^{2+}], it is not possible to quantify SSS change at our core site based on shell Ba/Ca ratios. Instead, we use the Ba/Ca record to identify periods when riverine input into the Gulf of Mexico was greater than the modern.

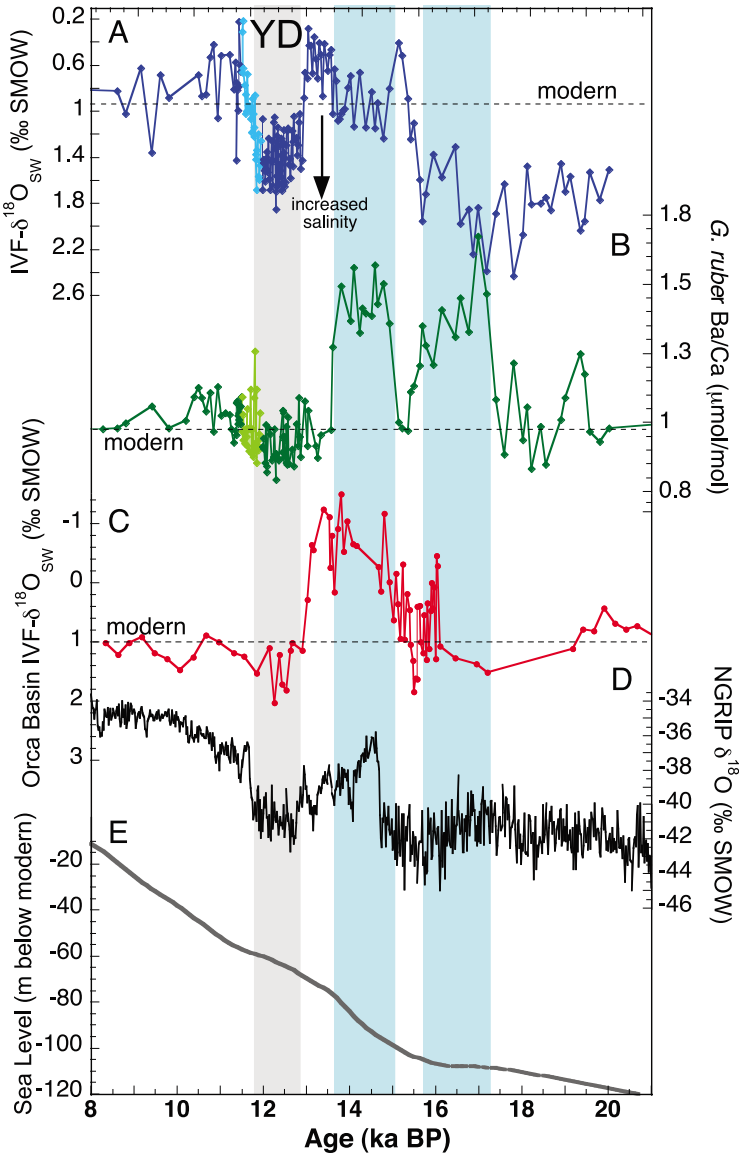

Figure 4. (a) Computed Florida Straits IVF-$\delta^{18}O_{SW}$ calculated from the Mg/Ca-derived SST and $\delta^{18}O_C$ using equation (2) [*Bemis et al.*, 1998]. The dashed horizontal line indicates the modern local $\delta^{18}O_{SW}$ value. (b) *G. ruber* Ba/Ca ratios in 26JPC. The predicted Ba/Ca ratio for a modern planktonic foraminifera living on the western margin of the Florida Straits is indicated by the horizontal dashed line. Intervals of increased riverine input as defined by elevated Ba/Ca are indicated by the blue shaded boxes. The data plotted in lighter shades in Figures 4a and 4b are from the interval in the core with the out of sequence radiocarbon ages. (c) Orca Basin (northern Gulf of Mexico) IVF-$\delta^{18}O_{SW}$ record from *Flower et al.* [2004]. Periods of increased meltwater into the Gulf of Mexico are characterized by highly depleted IVF-$\delta^{18}O_{SW}$ values. The modern $\delta^{18}O_{SW}$ value for the Orca Basin is indicated by the horizontal dashed line. (d) Oxygen isotopes in the NGRIP ice core showing the timing of colder conditions (low $\delta^{18}O$) in Greenland [*Andersen et al.*, 2004; *Rasmussen et al.*, 2006]. (e) Deglacial sea level change from *Siddall et al.* [2009]. Gray shaded region indicates the Younger Dryas.

[27] Alternatively, an additional source of dissolved barium is coastal sediments [*Moore*, 1999]. Barium adsorbed onto clays in a freshwater environment can desorb in saltwater as sea level rises across a continental shelf during a deglacial period. In addition, *Moore and Shaw* [1998] documented a release of dissolved barium in groundwater as saltwater encroached into previously freshwater aquifers in Florida. However, the first period of elevated *G. ruber* Ba/Ca ratios in 26JPC (17.2–15.6 ka BP) (Figure 4b) occurs during a pause in sea level rise from about 17.2–16.1 ka BP [*Siddall et al.*, 2009]. Although the second period of elevated Ba/Ca ratios (14.9–13.6 ka BP) does correspond to the first period of rapidly rising sea level across the deglacial, the abrupt decrease in Ba/Ca at 13.6 ka BP does not correspond with decreasing rates of sea level rise. Instead, sea level continued to rise through the YD, a period

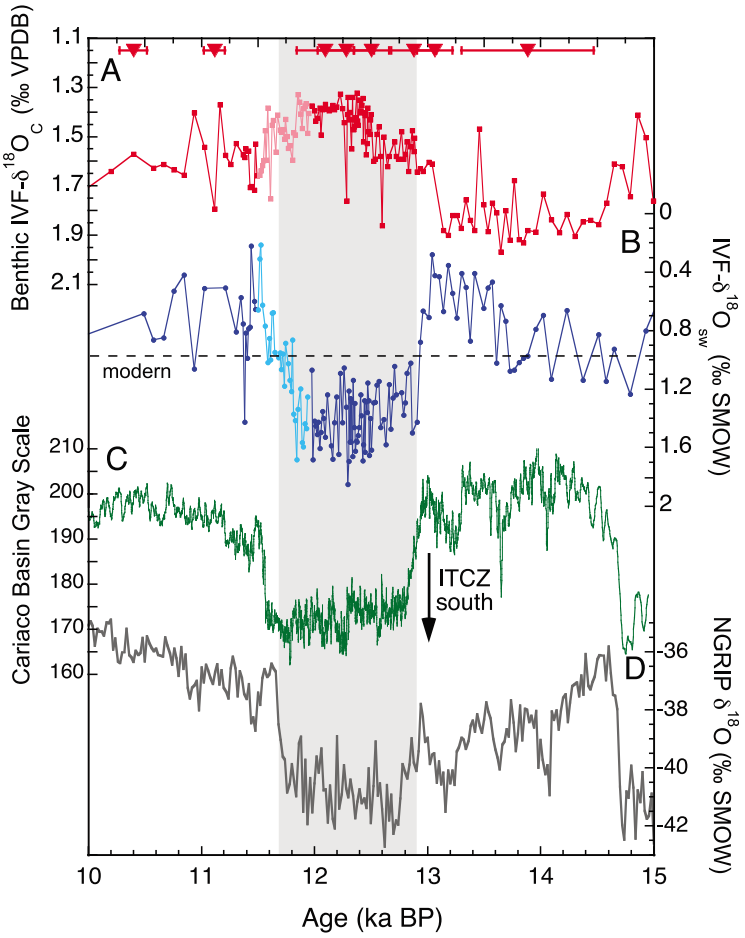

Figure 5. (a) Detail of the benthic (*C. pachyderma*) ice volume free $\delta^{18}O_C$ record from 26JPC [*Lynch-Stieglitz et al.*, 2011]. Low values during the Younger Dryas are interpreted as a reduction in the cross straits density gradient and reduced Florida Current flow. (b) The ice volume free $\delta^{18}O_{SW}$ record from 26JPC reconstructed from *G. ruber* using equations (1) and (2). The dashed horizontal line indicates the modern local $\delta^{18}O_{SW}$ value. The higher than modern values during the Younger Dryas reflect increased SSS during this interval. Data plotted in lighter shades in Figures 5a and 5b are from the interval in the core with the out of sequence radiocarbon ages. (c) Cariaco Basin gray scale record [*Hughen et al.*, 2004; *Hughen et al.*, 1998], reflecting variations in upwelling intensity associated with north-south migrations of the ITCZ. (d) Oxygen isotopes in the NGRIP ice core showing the timing of the Younger Dryas and colder conditions (low $\delta^{18}O$) in Greenland [*Andersen et al.*, 2004; *Rasmussen et al.*, 2006]. Gray shaded area denotes the Younger Dryas. Red triangles on the upper axis show the calibrated radiocarbon ages in this section of the core and their associated 2σ error.

marked by lower than modern Ba/Ca ratios in 26JPC. Given the close correspondence between elevated Ba/Ca ratios in 26JPC and negative $\delta^{18}O_{SW}$ values in the Orca Basin (Figures 4b and 4c), the most likely cause for elevated $[Ba^{2+}]$ in the Florida Straits is elevated riverine discharge into the Gulf of Mexico associated with periods of elevated Mississippi River runoff.

[28] Given the reported $[Ba^{2+}]$ in the modern Gulf of Mexico of 11.2 μg/L [*Hanor and Chan*, 1977] and the average Ba^{2+} concentration in the northern Caribbean is 8.5 μg/L [*Turekian and Johnson*, 1966], we estimate a modern $[Ba^{2+}]$ of 9.0 to 10.0 μg/L for the Florida Straits. Using the empirical relationship by *Lea and Spero* [1994], the calculated shell Ba/Ca ratio in equilibrium with this modern water mass would be ~0.95 μmol/mol. Using this value as a baseline to identify periods of elevated Ba^{2+} input into the Gulf of Mexico across the deglacial, the 26JPC Ba/Ca record indicates two prolonged periods when shell Ba/Ca ratios were significantly higher than the modern value: from 17.2 to 15.6 ka BP and 14.9 to 13.6 ka BP (blue boxes on Figure 4). The Orca Basin IVF-$\delta^{18}O_{SW}$ record [*Flower et al.*, 2004] also suggests two pulses of isotopically depleted meltwater into the Gulf of Mexico (Figure 4c). The decrease in the Orca Basin IVF-$\delta^{18}O_{SW}$ record starts 1 ka BP later than the initial rise in Ba/Ca ratios in 26JPC at 17.2 ka BP, but a new Orca Basin IVF-$\delta^{18}O_{SW}$ record based on the *Marion Dufresne* core MD02–2550 indicates the presence of isotopically depleted meltwater starting at ~17 ka BP [*Williams et al.*, 2010]. After 13.6 ka BP, Ba/Ca ratios in 26JPC drop to near modern values until 11.8 ka BP. On the transition out of the YD, a few intervals in the section of the core with the out of sequence ^{14}C dates show an increase in

Florida Straits [Ba^{2+}], but the increases are much less than those recorded in the period before the YD (Figure 4c).

[29] Therefore, we interpret the elevated Ba/Ca ratios starting at 17.2 ka BP and ending at 13.6 ka BP to constrain the period of increased riverine influence on Florida Straits surface waters from the melting of the Laurentide ice sheet. During this time, meltwater with depleted $\delta^{18}O$ values from the northern Gulf of Mexico mixed with Caribbean surface waters with a $\delta^{18}O_{SW}$ value near 0‰, making it difficult to constrain the $\delta^{18}O_{SW}$:SSS relationship for the Florida Straits. Nevertheless, it is interesting to note that the intervals with elevated Ba/Ca ratios (blue boxes on Figure 4) are not associated with highly depleted IVF-$\delta^{18}O_{SW}$ values. In fact, the rise in Ba/Ca at 17 ka BP corresponds to a period with the most enriched IVF-$\delta^{18}O_{SW}$ values (H1), suggesting that riverine input only had a minor impact on Florida Straits IVF-$\delta^{18}O_{SW}$ at this time. The enriched IVF-$\delta^{18}O_{SW}$ values during the early deglacial and H1 most likely reflect arid conditions in the tropical North Atlantic when the average position of the ITCZ was located south of its modern position.

[30] Regardless, geochemical and sedimentological evidence suggest that meltwater input into the Gulf of Mexico dramatically decreased to near modern levels by the start of the YD. Ba/Ca ratios in 26JPC decreased to modern values 600 years before the start of the YD, so the abrupt increase in Florida Straits IVF-$\delta^{18}O_{SW}$ values starting at 13.0 ka BP cannot be explained by an abrupt shut off of riverine input. Furthermore, IVF-$\delta^{18}O_{SW}$ values in the Orca Basin return to near modern values at 12.9 ka BP (Figure 4d), providing additional evidence that Mississippi River discharge had significantly diminished by the start of the YD. Additionally, two recent sedimentological studies from the Orca and Pigmy Basins suggest that Mississippi River discharge rates dramatically decreased by 12.9 ka BP and remained low through the YD interval [*Montero-Serrano et al.*, 2009; *Sionneau et al.*, 2010]. Therefore, the abrupt shift to heavier than modern IVF-$\delta^{18}O_{SW}$ values at the start of the YD probably reflects an increase in Florida Straits surface salinity resulting from increased regional E/P ratios.

4.4. Estimating Sea Surface Salinity Change Across the Younger Dryas

[31] Based on the modern tropical Atlantic $\delta^{18}O_{SW}$:SSS relationship (see above), the IVF-$\delta^{18}O_{SW}$ increase of 0.43 ‰ above modern values from 13.04–12.91 ka BP would indicate a SSS increase of +1.7 in about 130 years. However, the assumption that the modern $\delta^{18}O_{SW}$:SSS relationship was the same during the YD is probably not valid. The results of an oxygen isotope-enabled GCM hosing experiment show a significant decrease in precipitation $\delta^{18}O$ values over the Caribbean and Gulf of Mexico associated with an AMOC-related cooling in the North Atlantic [*Lewis et al.*, 2010]. This is because the amount effect leads to an enrichment in precipitation $\delta^{18}O$ values associated with the ITCZ, so the southward shift of the ITCZ during cool phases in the North Atlantic results in an increase in precipitation $\delta^{18}O$ values over the tropical South Atlantic and a decrease in precipitation $\delta^{18}O$ values in the Caribbean (by about −2‰) [*Lewis et al.*, 2010]. A decrease of −2‰ in the freshwater end-member would increase the slope of the regional $\delta^{18}O_{SW}$:SSS relationship to about 0.32, therefore reducing the magnitude of the estimated SSS increase to +0.85. However, because it is not possible to determine changes in past freshwater end-member values with certainty, any estimates of actual SSS change based on calculated $\delta^{18}O_{SW}$ values should be viewed with caution. Instead, we interpret the IVF-$\delta^{18}O_{SW}$ record to indicate periods when SSS was most likely saltier or fresher relative to the modern.

[32] The abrupt increase in IVF-$\delta^{18}O_{SW}$ values at the start of the YD occurs within 10 cm or 130 years (Figure 5a). The midpoint of this transition is at 13.0 ka BP (±199 years) and is within age model error of the start of the YD in the NGRIP $\delta^{18}O$ ice core record (12.896 ka BP; ±138 years) (Figure 5d). Although the transition out of the YD occurs within the section of 26JPC with the out of sequence ^{14}C dates, this transition is also rapid, occurring within 200 years with a midpoint at 11.73 ka BP. In the NGRIP $\delta^{18}O$ ice core record, the transition at the end of the YD occurs at 11.703 ka BP (maximum counting error of 99 years) [*Rasmussen et al.*, 2006]. It is encouraging that the IVF-$\delta^{18}O_{SW}$ transition in 26JPC at the end of the YD is synchronous (within age model error) with the NGRIP $\delta^{18}O$ record, suggesting that whatever process caused the anomalous ^{14}C-dated intervals did not compromise this entire section of 26JPC.

4.5. Multivariate SST and SSS Reconstructions

[33] Although both culturing studies [*Kisakürek et al.*, 2008; *Lea et al.*, 1999; *Mashiotta et al.*, 1999; *Nürnberg et al.*, 1996; *Russell et al.*, 2004] as well as core top and sediment trap studies [*Anand et al.*, 2003; *Dekens et al.*, 2002; *Elderfield and Ganssen*, 2000; *Hastings et al.*, 1998; *Lea et al.*, 2000; *McConnell and Thunell*, 2005; *McKenna and Prell*, 2004; *Rosenthal et al.*, 1997, 2000] show that temperature is the primary control of Mg/Ca ratios in foraminiferal calcite, recent studies found a relationship between Mg/Ca ratios in core top planktonic foraminifera and salinity [*Arbuszewski et al.*, 2010; *Ferguson et al.*, 2008; *Mathien-Blard and Bassinot*, 2009]. By analyzing Mg/Ca and $\delta^{18}O_C$ in core tops across an Atlantic meridional transect, *Arbuszewski et al.* [2010] developed new multivariate equations to calculate mean annual SST and SSS that take into account the effect of salinity on shell Mg/Ca. Their new multivariate equations use both the measured shell Mg/Ca ratio and $\delta^{18}O_C$ value to calculate SST and SSS:

$$\mathrm{SST}(^{\circ}\mathrm{C}) = 16.06 + 4.62^{*}\ln(\mathrm{Mg/Ca}) - 3.42\left(\delta^{18}O_C\right) - 0.1\left(\Delta CO_3^{2-}\right) \quad (3)$$

$$\mathrm{SSS} = 34.28 + 1.97^{*}\ln(\mathrm{Mg/Ca}) + 0.59(\delta^{18}O_C) \quad (4)$$

Analytical uncertainty in our record contributes an additional error of ±0.44°C when calculating SST using multivariate equation (3). When calculating SSS using multivariate equation (4), analytical uncertainty contributes an additional error of ±0.12.

[34] *Arbuszewski et al.* [2010] found a 27% increase in shell Mg/Ca per 1 salinity unit increase when SSS was above 35. Although it is still not clear why elevated SSS would have such a large impact on shell Mg/Ca ratios, we wanted to determine how *Arbuszewski et al.*'s [2010] newly proposed

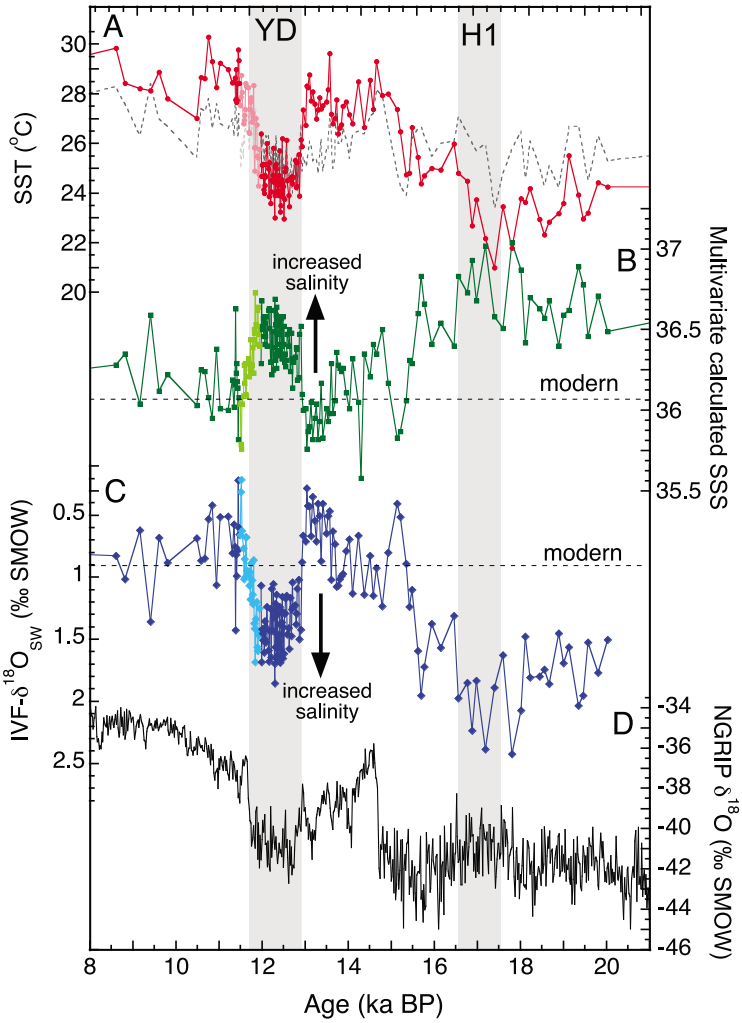

Figure 6. (a) A comparison of the deglacial SST record calculated using the multivariate equation (3) by *Arbuszewski et al.* [2010] (solid line with circles) and the traditional equation (1) from *Anand et al.* [2003] (dashed gray line). (b) SSS calculated using the multivariate equation (4) by *Arbuszewski et al.* [2010]. The influence of global $\delta^{18}O_{SW}$ change due to continental ice volume variation [*Siddall et al.*, 2009] has been removed, so the SSS values are ice volume corrected. The horizontal dashed line indicates the modern mean annual SSS at our study site. (c) Computed IVF-$\delta^{18}O_{SW}$ calculated using the traditional method from the Mg/Ca-derived SST and $\delta^{18}O_C$ using equation (2) [*Bemis et al.*, 1998]. The dashed horizontal line indicates the modern local $\delta^{18}O_{SW}$ value. Note the reverse axis with positive down. (d) Oxygen isotopes in the NGRIP ice core showing the timing of colder conditions (low $\delta^{18}O$) in Greenland [*Andersen et al.*, 2004; *Rasmussen et al.*, 2006]. Shaded regions indicate the Younger Dryas (YD) and Heinrich Event 1 (H1), and the data plotted in lighter shades are from the interval in the core with the out of sequence radiocarbon ages.

multivariate equations would affect our results. Therefore, we recalculated deglacial SST and SSS change using equations (3) and (4) and compare the results with those obtained using equations (1) and (2) (Figure 6). Given the shallow depth of 26JPC, we did not include the correction factor to account for changes in ΔCO_3^{2-} in equation (3).

[35] In order to calculate SST using the multivariate equation (3), both $\delta^{18}O_C$ and Mg/Ca measurements on an interval are required. The youngest interval in 26JPC with both measurements is at 96.25 cm (6.13 ka BP). The estimated SST for this interval based on equation (3) is 28.7°C, or 1.8°C above the modern mean value. For comparison, the calculated SST for this interval using equation (1) is 27.2°C. The coolest temperatures calculated using equation (3) occur from 17.2 to 17.8 ka BP when minimum SSTs are calculated to have decreased to ~22°C (Figure 6a). Taken at face value, the multivariate SST equation (3) suggests a temperature gradient as large as 6.7°C across the deglacial, much larger than the estimated cooling of only ~3°C in the Florida Straits at the LGM based on the results of the MARGO project [*Waelbroeck et al.*, 2009]. Both equations (1) and (3) suggest similar warm conditions at the start of the BA around 14.5 ka BP. However, the multivariate equation (3) indicates SSTs remained relatively warm until the start of the YD at 13.0 ka BP when SST rapidly decreased by 4.4°C. Multivariate equation (3) calculates an average SST of

24.4°C from 12.9 to 12.2 ka BP (0.7°C cooler than SSTs calculated for this interval using equation (1)). Therefore, use of multivariate equation (3) results in a very large, abrupt temperature decrease in the Florida Straits at the start of the YD rather than the gradual cooling calculated by equation (1). Because coupled GCM water hosing experiments predict a relatively small SST response (<2°C) in the Florida Straits, even when AMOC is reduced by 75% [*Zhang and Delworth*, 2005], the abrupt 4.4°C SST decrease in the Florida Straits calculated using multivariate equation (3) at the start of the YD is larger than what most regional climate reconstructions and modeling experiments suggest is reasonable.

[36] For comparison, we also calculate SSS change in 26JPC across the deglacial using multivariate equation (4) [*Arbuszewski et al.*, 2010] (Figure 6b). In order to construct this SSS record, we used the same correction for the influence of global $\delta^{18}O_{SW}$ change due to continental ice volume variation [*Siddall et al.*, 2009], so the estimated SSS values on Figure 6b are ice volume free. Importantly, the timing of deglacial SSS change calculated using the multivariate equation is the same as the reconstructed IVF-$\delta^{18}O_{SW}$ change using equations (1) and (2) (Figures 6b and 6c). The periods prior to 15.5 ka BP and the YD stand out as the saltiest (and most positive IVF-$\delta^{18}O_{SW}$ values) periods in the record. The section of the core associated with H1 indicates a period of maximum SSS when the average salinity was 36.8 (0.7 higher than modern). Surface salinity then decreased at ~15 ka BP and remained fresher or similar to modern values until 13.0 ka BP when the start of the YD is marked by an abrupt increase in SSS. Although the timing of the salinity increase is the same using multivariate equation (4), the magnitude of SSS increase is only +0.4 (Figure 6b).

[37] Because a change in the slope of the regional $\delta^{18}O_{SW}$: SSS relationship would also affect accuracy of the multivariate SSS calculation, the actual SSS values calculated using either the traditional or multivariate equations should only be viewed as estimates. Regardless, both surface water salinity reconstructions (Figures 6b and 6c) indicate a rapid shift to saltier conditions at the start of the YD.

4.6. Paired Planktonic-Benthic Oxygen Isotopes in 26JPC

[38] *Lynch-Stieglitz et al.* [2011] measured $\delta^{18}O$ in benthic foraminifera from a suite of cores (including 26JPC) located on both margins of the Florida Straits for the past 15 ka BP. They found that the contrast in benthic $\delta^{18}O$ tests across the Florida Straits was reduced during the YD, most likely reflecting a reduction in the density gradient across the channel and a decrease in the vertical shear of the Florida Current at that time. Their results are consistent with a significant weakening of the Florida Current resulting from reduced flow of the surface branch of AMOC, similar to the magnitude of AMOC reduction *Lynch-Stieglitz et al.* [1999] estimated for the LGM.

[39] Furthermore, *Lynch-Stieglitz et al.* [2011] argued the high-resolution 26JPC benthic IVF-$\delta^{18}O_C$ record can be used to determine the timing of Florida Current flow variability across the YD (Figure 5a). Therefore, the abrupt decrease in benthic IVF-$\delta^{18}O_C$ at the start of the YD (within 4 cm or 78 years) reflects a dramatic change in ocean circulation at the start of the YD, consistent with a significant reduction of AMOC. In comparison, the abrupt increase in IVF-$\delta^{18}O_{SW}$ values at the start of the YD occurs within 10 cm or 130 years (Figures 5a and 5b). Although age model uncertainty does not allow us to quantify the exact duration of these transitions, the more rapid benthic IVF-$\delta^{18}O_C$ transition in our records suggests that Florida Current transport has the potential to adjust faster than atmospheric-induced surface water salinity change in the tropics.

[40] The midpoint of the 26JPC benthic IVF-$\delta^{18}O_C$ changes occurs 9 cm or about 100 years before the midpoint of the increase in IVF-$\delta^{18}O_{SW}$ (Figure 5b). However, *McCorkle et al.* [1997] showed that the benthic species *C. pachyderma* can live in burrows within the sediment. This may result in an offset of several centimeters in the core relative to coeval planktonic foraminiferal species. Therefore, it is not possible to definitively determine if ocean circulation changes recorded by the benthic foraminifera preceded or are concurrent with the rapid increase in Florida Straits SSS recorded by the planktonic foraminifera at the start of the YD. Nevertheless, the nearly synchronous changes in both records are consistent with an abrupt reorganization of tropical Atlantic atmospheric circulation in response to a meltwater-induced reduction in AMOC at the start of the YD. If ocean circulation changes were the main driver of IVF-$\delta^{18}O_{SW}$ change in the Florida Straits, we would expect a more gradual buildup of salt that would continue to increase as long as AMOC remained in a reduced state.

[41] In comparison, the timing of the IVF-$\delta^{18}O_{SW}$ transition at the end of the YD precedes the more gradual ocean circulation recovery recorded by the benthic foraminifera. The decrease in IVF-$\delta^{18}O_{SW}$ values occurs in about 200 years and is complete by 11.62 ka BP (±250 years) at 364 cm in the core. In contrast, the benthic IVF-$\delta^{18}O_C$ increase takes over 350 years and is not complete until 11.47 ka BP (±250 years) at 340 cm in the core. These results suggest atmospheric circulation returned to a pre-YD mode before AMOC fully recovered. If correct, these results suggest a lead in atmospheric circulation change on interstadial transitions.

4.7. Tropical Atmospheric Circulation Change and High Latitude Climate

[42] Several studies interpret sedimentological and geochemical changes in the Cariaco Basin to indicate a coupled high- to low-latitude climate linkage over the last glacial cycle [*Haug et al.*, 2001, 2003; *Hughen et al.*, 1998; *Peterson et al.*, 2000; *Peterson and Haug*, 2006]. Variations in the trace metal content and color variations recorded in 'gray scale' of Cariaco Basin sediment cores indicate a synchronous shift to drier conditions in the western tropical Atlantic at the onset of the YD. In particular, the gray scale record [*Hughen et al.*, 2004, 1996, 1998] indicates an abrupt shift to lighter values at 12.85 ka BP (Figure 5c), reflecting enhanced upwelling and stronger trade winds as the ITCZ shifted southward in response to a cooling in the North Atlantic. The abrupt increase in 26JPC IVF-$\delta^{18}O_{SW}$ values at the start of the YD is synchronous (within age model error) with the Cariaco record. Because Florida Current surface salinity is strongly influenced by E/P changes in the Caribbean and tropical Atlantic, the most likely cause of the elevated IVF-$\delta^{18}O_{SW}$ values at the start of the YD is a combination of increased evaporation (due to stronger trade winds) and/or

decreased tropical Atlantic precipitation. As the Hadley Cells and the corresponding position of the ITCZ shifted southward at the start of the YD, the tropical Atlantic hydrologic cycle shifted into a stable stadial mode characterized by increased surface water salinity in the Florida Straits.

[43] This conclusion is also supported by coupled GCM water hosing simulations of AMOC weakening. The resulting high-latitude cooling shifts the ITCZ southward and strengthens the NE trade winds [*Dahl et al.*, 2005; *Krebs and Timmermann*, 2007a, 2007b; *Lohmann*, 2003; *Stouffer et al.*, 2006; *Vellinga and Wood*, 2002; *Zhang and Delworth*, 2005]. These atmospheric circulation changes result in a precipitation deficit in the tropical/subtropical North Atlantic and the development of a positive salinity anomaly in the northern tropical Atlantic that ultimately increases the upper-ocean density in the deep-water formation regions of the North Atlantic, thereby playing an important role in accelerating the recovery of AMOC [*Krebs and Timmermann*, 2007a, 2007b; *Vellinga and Wu*, 2004]. In another modeling study, *Wan et al.* [2010] showed that atmospheric processes are primarily responsible for the increase in tropical North Atlantic SSS during periods of reduced AMOC, while ocean circulation changes result in increased surface salinity in the equatorial and southern tropical Atlantic. Therefore, the rapid increase in IVF-$\delta^{18}O_{SW}$ values in the Florida Straits at the start of the YD is most likely caused by the tropical hydrologic cycle's response to high-latitude cooling.

[44] Using Mg/Ca and alkenone paleothermometry along with oxygen isotope measurements on planktonic foraminifera, *Benway et al.* [2006] and *Leduc et al.* [2007] reconstructed deglacial $\delta^{18}O_{SW}$ change in the eastern equatorial Pacific (EEP) and estimated a YD salinity increase that was 2–3 times larger than those estimated for the YD Caribbean [*Schmidt et al.*, 2004]. In their study, *Leduc et al.* [2007] argued for decreased water vapor transport from the Atlantic to the Pacific during the YD and Heinrich events. However, it is not appropriate to directly compare the *Leduc et al.* [2007] and *Schmidt et al.* [2004] $\delta^{18}O_{SW}$ reconstructions because of resolution differences between the records. Sedimentation rates at the *Leduc et al.* [2007] study site are 10 times higher than those in the Colombian Basin, so the true magnitude of Caribbean $\delta^{18}O_{SW}$ change has most likely been smoothed by bioturbation. However, a comparison of the *Leduc et al.* [2007] data with our new high-resolution JPC26 IVF-$\delta^{18}O_{SW}$ record from the Florida Straits shows similar IVF-$\delta^{18}O_{SW}$ increases at both study sites at the start of the YD. Therefore, the elevated IVF-$\delta^{18}O_{SW}$ values in both the western tropical North Atlantic and in the northern EEP probably reflect a southward shift in the ITCZ during the YD and a drier climate in both regions.

[45] Our new results also suggest the planktonic-based IVF-$\delta^{18}O_{SW}$ record returns to pre-YD values before the benthic-based IVF-$\delta^{18}O_C$ record indicates a full recovery of Florida Current transport. This implies that atmospheric circulation changes may have preceded large-scale ocean circulation changes on transitions into warm intervals. A recent geochemical and sedimentological study of a well-dated lake core from the Venezuelan Andes also found evidence for an early tropical Atlantic warming during the YD that began several hundred years before the termination of the event in the high latitudes [*Stansell et al.*, 2010]. Additionally, a recent GCM hosing experiment using glacial boundary conditions found that the ITCZ recovers from its southward displacement before AMOC fully recovers [*Otto-Bliesner and Brady*, 2010]. The 26JPC IVF-$\delta^{18}O_{SW}$ record may be further evidence for a lead in tropical atmospheric circulation change on interstadial transitions. Nevertheless, this conclusion must be viewed with caution because this transition is located within the section of 26JPC that may have disturbed intervals.

5. Conclusions

[46] Based on Mg/Ca paleothermometry and oxygen isotope measurements on the planktonic foraminifera *G. ruber* in Florida Straits sediment core 26JPC, we reconstructed a high-resolution record of IVF-$\delta^{18}O_{SW}$ change for the last 21 ka BP. In addition, we measured Ba/Ca ratios in *G. ruber* shell material as a proxy for large meltwater injections into the Gulf of Mexico across the deglacial. We have shown that the surface water $\delta^{18}O$ values in the Florida Straits were most likely influenced by isotopically depleted riverine input from 17.2 to 15.6 ka BP and 14.9 to 13.6 ka BP, complicating the estimation of SSS change based on the IVF-$\delta^{18}O_{SW}$ record during these intervals. However, Ba/Ca ratios in the 26JPC record decreased about 600 years before the start of the YD, suggesting a greatly diminished riverine component in Florida Straits surface water at this time.

[47] The transition into the YD cold interval is marked by an abrupt increase in Florida Straits IVF-$\delta^{18}O_{SW}$ values that occurs within 130 years. This rapid increase in IVF-$\delta^{18}O_{SW}$ is synchronous (within age model error) with atmospheric circulation changes recorded in both the high-latitude NGRIP $\delta^{18}O$ ice core record and the low-latitude Cariaco Basin gray scale record. Therefore, the most likely explanation for the elevated IVF-$\delta^{18}O_{SW}$ values at the start of the YD is an abrupt shift in atmospheric circulation that resulted in a net increase in evaporation and/or net decrease in precipitation in the tropical Atlantic. Furthermore, we compared the timing of surface water changes in 26JPC to a recently published record of Florida Current variability in the same core based on benthic oxygen isotope data [*Lynch-Stieglitz et al.*, 2011]. Our results indicate nearly synchronous changes in atmospheric and ocean circulation on the transition into the YD. These results are consistent with an abrupt reduction in AMOC as the driver of tropical atmospheric circulation at the start of the YD. Furthermore, the pattern of reduced AMOC and elevated surface water salinity in the tropical Atlantic seems to be consistent across both millennial and orbital time scales [*Schmidt et al.*, 2004], suggesting that meridional shifts in the ITCZ forced by North Atlantic climate are a robust feature of the climate system.

[48] **Acknowledgments.** We thank the National Science Foundation (grants OCE-0823498 (M.W.S.) and OCE-0648258 and OCE-0096472 (J.L.S.)) for supporting this research. A NOAA Global Change Postdoctoral Fellowship also supported M.W.S. We thank Tiee-Yuh Chang, Amy Gondran, and Franco Marcantonio for technical help.

References

Alley, R., and P. U. Clark (1999), The glaciation of the northern hemisphere: A global perspective, *Annu. Rev. Earth Planet. Sci.*, *27*, 149–182, doi:10.1146/annurev.earth.27.1.149.

Anand, P., H. Elderfield, and M. H. Conte (2003), Calibration of Mg/Ca thermometry in planktonic foraminifera from a sediment trap time series, *Paleoceanography*, *18*(2), 1050, doi:10.1029/2002PA000846.

Andersen, K. K., et al. (2004), High-resolution record of Northern Hemisphere climate extending into the last interglacial period, *Nature*, *431*(7005), 147–151, doi:10.1038/nature02805.

Antonov, J. I., D. Seidov, T. P. Boyer, R. A. Locarnini, A. V. Mishonov, and H. E. Garcia (Eds.) (2010), *World Ocean Atlas 2009*, 184 pp., U.S. Gov. Print. Off., Washington, D. C.

Arbuszewski, J., P. deMenocal, A. Kaplan, and E. Farmer (2010), On the fidelity of shell-derived δ^{18}O seawater estimates, *Earth Planet. Sci. Lett.*, *300*, 185–196, doi:10.1016/j.epsl.2010.10.035.

Bemis, B. E., H. J. Spero, J. Bijima, and D. W. Lea (1998), Reevaluation of the oxygen isotopic composition of planktonic foraminifera: Experimental results and revised paleotemperature equations, *Paleoceanography*, *13*(2), 150–160, doi:10.1029/98PA00070.

Benway, H. M., A. C. Mix, B. A. Haley, and G. P. Klinkhammer (2006), Eastern Pacific Warm Pool paleosalinity and climate variability: 0–30 kyr, *Paleoceanography*, *21*, PA3008, doi:10.1029/2005PA001208.

Boyle, E. A. (2000), Is ocean thermohaline circulation linked to abrupt stadial/interstadial transitions?, *Quat. Sci. Rev.*, *19*, 255–272, doi:10.1016/S0277-3791(99)00065-7.

Bradley, R. S., and J. H. England (2008), The Younger Dryas and the sea of ancient ice, *Quat. Res.*, *70*(1), 1–10, doi:10.1016/j.yqres.2008.03.002.

Broecker, W. S., J. P. Kennett, B. P. Flower, J. T. Teller, S. Trumbore, G. Bonani, and W. Wolfli (1989), Routing of meltwater from the Laurentide Ice-Sheet during the Younger Dryas cold episode, *Nature*, *341*(6240), 318–321, doi:10.1038/341318a0.

Broecker, W. S., G. Bond, M. Klas, G. Bonani, and W. Wolfli (1990), A salt oscillator in the glacial Atlantic? The concept, *Paleoceanography*, *5*(4), 469–478, doi:10.1029/PA005i004p00469.

Carlson, A. E., D. W. Oppo, R. E. Came, A. N. LeGrande, L. D. Keigwin, and W. B. Curry (2008), Subtropical Atlantic salinity variability and Atlantic meridional circulation during the last deglaciation, *Geology*, *36*(12), 991–994, doi:10.1130/G25080A.1.

Chang, P., R. Zhang, W. Hazeleger, C. Wen, X. Q. Wan, L. Ji, R. J. Haarsma, W. P. Breugem, and H. Seidel (2008), Oceanic link between abrupt changes in the North Atlantic Ocean and the African monsoon, *Nat. Geosci.*, *1*(7), 444–448, doi:10.1038/ngeo218.

Charles, C. D., and R. G. Fairbanks (1990), Glacial to interglacial changes in the isotopic gradients of southern ocean surface water, in *Geological History of the Polar Oceans: Arctic Versus Antarctic*, edited by U. Bleil and J. Thiede, pp. 519–538, Kluwer Acad., Dordrecht, Netherlands.

Chiang, J. C. H., W. Cheng, and C. M. Bitz (2008), Fast teleconnections to the tropical Atlantic sector from Atlantic thermohaline adjustment, *Geophys. Res. Lett.*, *35*, L07704, doi:10.1029/2008GL033292.

Coffey, M., F. Dehairs, O. Collette, G. Luther, T. Church, and T. Jickells (1997), The behaviour of dissolved barium in estuaries, *Estuarine Coastal Shelf Sci.*, *45*(1), 113–121, doi:10.1006/ecss.1996.0157.

Dahl, K., A. Broccoli, and R. Stouffer (2005), Assessing the role of North Atlantic freshwater forcing in millennial scale climate variability: A tropical Atlantic perspective, *Clim. Dyn.*, *24*(4), 325–346, doi:10.1007/s00382-004-0499-5.

Dekens, P. S., D. W. Lea, D. K. Pak, and H. J. Spero (2002), Core top calibration of Mg/Ca in tropical foraminifera: Refining paleotemperature estimation, *Geochem. Geophys. Geosyst.*, *3*(4), 1022, doi:10.1029/2001GC000200.

Edmond, J. M., E. D. Boyle, D. Drummond, B. Grant, and T. Mislick (1978), Desorption of barium in the plume of the Zaire (Congo) River, *Neth. J. Sea Res.*, *12*(3–4), 324–328, doi:10.1016/0077-7579(78)90034-0.

Elderfield, H., and G. Ganssen (2000), Past temperature and δ^{18}O of surface ocean waters inferred from foraminiferal Mg/Ca ratios, *Nature*, *405*, 442–445, doi:10.1038/35013033.

Fairbanks, R. G. (1989), A 17,000-year glacio-eustatic sea level record: Influence of glacial melting rates on the Younger Dryas event and deep-ocean circulation, *Nature*, *342*, 637–642, doi:10.1038/342637a0.

Ferguson, J. E., G. M. Henderson, M. Kucera, and R. E. M. Rickaby (2008), Systematic change of foraminiferal Mg/Ca ratios across a strong salinity gradient, *Earth Planet. Sci. Lett.*, *265*(1–2), 153–166, doi:10.1016/j.epsl.2007.10.011.

Flower, B. P., D. W. Hastings, H. W. Hill, and T. M. Quinn (2004), Phasing of deglacial warming and Laurentide Ice Sheet meltwater in the Gulf of Mexico, *Geology*, *32*(7), 597–600, doi:10.1130/G20604.1.

Fratantoni, P. S., T. N. Lee, G. P. Podesta, and F. Muller-Karger (1998), The influence of Loop Current perturbations on the formation and evolution of Tortugas eddies in the southern Straits of Florida, *J. Geophys. Res.*, *103*, 24,759–24,779, doi:10.1029/98JC02147.

Guilderson, T. P., R. G. Fairbanks, and J. L. Rubenstone (2001), Tropical Atlantic coral oxygen isotopes: Glacial-interglacial sea surface temperatures and climate change, *Mar. Geol.*, *172*, 75–89, doi:10.1016/S0025-3227(00)00115-8.

Hall, J. M., and L. H. Chan (2004), Ba/Ca in *Neogloboquadrina pachyderma* as an indicator of deglacial meltwater discharge into the western Arctic Ocean, *Paleoceanography*, *19*, PA1017, doi:10.1029/2003PA000910.

Hanor, J. S., and L. H. Chan (1977), Non-conservative behavior of barium during mixing of Mississippi River and Gulf of Mexico waters, *Earth Planet. Sci. Lett.*, *37*, 242–250, doi:10.1016/0012-821X(77)90169-8.

Hastings, D. W., A. D. Russell, and S. R. Emerson (1998), Foraminiferal magnesium in *Globigerinoides sacculifer* as a paleotemperature proxy, *Paleoceanography*, *13*(2), 161–169, doi:10.1029/97PA03147.

Haug, G. H., K. A. Hughen, D. M. Sigman, L. C. Peterson, and U. Rohl (2001), Southward migration of the intertropical convergence zone through the Holocene, *Science*, *293*, 1304–1308, doi:10.1126/science.1059725.

Haug, G. H., D. Gunther, L. C. Peterson, D. M. Sigman, K. A. Hughen, and B. Aeschlimann (2003), Climate and the collapse of Maya Civilization, *Science*, *299*, 1731–1735, doi:10.1126/science.1080444.

Hönisch, B., K. A. Allen, A. D. Russell, S. M. Eggins, J. Bijma, H. J. Spero, D. W. Lea, and J. Yu (2011), Planktic foraminifers as recorders of seawater Ba/Ca, *Mar. Micropaleontol.*, *79*, 52–57, doi:10.1016/j.marmicro.2011.01.003.

Hughen, K. A., J. T. Overpeck, L. C. Peterson, and S. E. Trumbore (1996), Rapid climate changes in the tropical Atlantic region during the last deglaciation, *Nature*, *380*, 51–54, doi:10.1038/380051a0.

Hughen, K. A., J. T. Overpeck, S. J. Lehman, M. Kashgarian, J. Southon, L. C. Peterson, R. Alley, and D. M. Sigman (1998), Deglacial changes in ocean circulation from an extended radiocarbon calibration, *Nature*, *391*, 65–68, doi:10.1038/34150.

Hughen, K., S. Lehman, J. Southon, J. Overpeck, O. Marchal, C. Herring, and J. Turnbull (2004), C-14 activity and global carbon cycle changes over the past 50,000 years, *Science*, *303*(5655), 202–207, doi:10.1126/science.1090300.

Hüls, M., and R. Zahn (2000), Millennial-scale sea surface temperature variability in the western tropical North Atlantic from planktonic foraminiferal census counts, *Paleoceanography*, *15*(6), 659–678, doi:10.1029/1999PA000462.

Kennett, J. P., and N. J. Shackleton (1975), Laurentide Ice Sheet meltwater recorded in Gulf of Mexico deep-sea cores, *Science*, *188*, 147–150, doi:10.1126/science.188.4184.147.

Kisakürek, B., A. Eisenhauer, F. Bohm, D. Garbe-Schonberg, and J. Erez (2008), Controls on shell Mg/Ca and Sr/Ca in cultured planktonic foraminiferan, Globigerinoides ruber (white), *Earth Planet. Sci. Lett.*, *273*(3–4), 260–269, doi:10.1016/j.epsl.2008.06.026.

Krebs, U., and A. Timmermann (2007a), Tropical air–sea interactions accelerate the recovery of the Atlantic Meridional Overturning Circulation after a major shutdown, *J. Clim.*, *20*, 4940–4956, doi:10.1175/JCLI4296.1.

Krebs, U., and A. Timmermann (2007b), Fast advective recovery of the Atlantic meridional overturning circulation after a Heinrich event, *Paleoceanography*, *22*, PA1220, doi:10.1029/2005PA001259.

Lea, D. W., and P. A. Martin (1996), A rapid mass spectrometric method for the simultaneous analysis of barium, cadmium, and strontium in foraminifera shells, *Geochim. Cosmochim. Acta*, *60*(16), 3143–3149, doi:10.1016/0016-7037(96)00184-6.

Lea, D. W., and H. J. Spero (1994), Assessing the reliability of paleochemical tracers: Barium uptake in the shells of planktonic formainifera, *Paleoceanography*, *9*(3), 445–452, doi:10.1029/94PA00151.

Lea, D. W., T. A. Mashiotta, and H. J. Spero (1999), Controls on magnesium and strontium uptake in planktonic foraminifera determined by live culturing, *Geochim. Cosmochim. Acta*, *63*(16), 2369–2379, doi:10.1016/S0016-7037(99)00197-0.

Lea, D. W., D. K. Pak, and H. J. Spero (2000), Climate impact of Late Quaternary equatorial Pacific sea surface temperature variations, *Science*, *289*, 1719–1724, doi:10.1126/science.289.5485.1719.

Lea, D. W., D. K. Pak, L. C. Peterson, and K. A. Hughen (2003), Synchroneity of tropical high latitude Atlantic temperatures over the last glacial termination, *Science*, *301*, 1361–1364, doi:10.1126/science.1088470.

Leduc, G., L. Vidal, K. Tachikawa, F. Rostek, C. Sonzogni, L. Beaufort, and E. Bard (2007), Moisture transport across Central America as a positive feedback on abrupt climatic changes, *Nature*, *445*(7130), 908–911, doi:10.1038/nature05578.

Lee, T. N., K. Leamann, E. Williams, T. Berger, and L. Atkinson (1995), Florida Current meanders and gyre formation in the southern Straits of Florida, *J. Geophys. Res.*, *100*, 8607–8620, doi:10.1029/94JC02795.

Lewis, S. C., A. N. LeGrande, M. Kelley, and G. A. Schmidt (2010), Water vapour source impacts on oxygen isotope variability in tropical precipitation during Heinrich events, *Clim. Past*, *6*(3), 325–343, doi:10.5194/cp-6-325-2010.

Locarnini, R. A., A. V. Mishonov, J. I. Antonov, T. P. Boyer, and H. E. Garcia (2006), *World Ocean Atlas 2005*, vol. 1, *Temperature*, *NOAA Atlas NESDIS*, vol. 61, edited by S. Levitus, 182 pp., NOAA, Silver Spring, Md.

Lohmann, G. (2003), Atmospheric and oceanic freshwater transport during weak Atlantic overturning circulation, *Tellus Ser. A*, *55*, 438–449.

Lohmann, G., and S. Lorenz (2000), The water cycle under paleoclimatic conditions as derived from AGCM simulations, *J. Geophys. Res.*, *105*, 17,417–17,436, doi:10.1029/2000JD900189.

Lund, D. C., and W. Curry (2006), Florida Current surface temperature and salinity variability during the last millennium, *Paleoceanography*, *21*, PA2009, doi:10.1029/2005PA001218.

Lynch-Stieglitz, J., W. B. Curry, and N. Slowey (1999), Weaker Gulf Stream in the Florida Straits during the Last Glacial Maximum, *Nature*, *402*(6762), 644–648, doi:10.1038/45204.

Lynch-Stieglitz, J., M. W. Schmidt, and W. B. Curry (2011), Evidence from the Florida Straits for Younger Dryas Ocean Circulation Changes, *Paleoceanography*, *26*, PA1205, doi:10.1029/2010PA002032.

Mashiotta, T. A., D. W. Lea, and H. J. Spero (1999), Glacial-interglacial changes in subantarctic sea surface temperature and δ^{18}O-water using foraminiferal Mg, *Earth Planet. Sci. Lett.*, *170*, 417–432, doi:10.1016/S0012-821X(99)00116-8.

Mathien-Blard, E., and F. Bassinot (2009), Salinity bias on the foraminifera Mg/Ca thermometry: Correction procedure and implications for past ocean hydrographic reconstructions, *Geochem. Geophys. Geosyst.*, *10*, Q12011, doi:10.1029/2008GC002353.

Maul, G., and F. M. Vukovich (1993), The relationship between variations in the Gulf of Mexico Loop Current and Straits of Florida volume transport, *J. Phys. Oceanogr.*, *23*, 785–796, doi:10.1175/1520-0485(1993)023<0785:TRBVIT>2.0.CO;2.

McConnell, M. C., and R. C. Thunell (2005), Calibration of the planktonic foraminiferal Mg/Ca paleothermometer: Sediment trap results from the Guaymas Basin, Gulf of California, *Paleoceanography*, *20*, PA2016, doi:10.1029/2004PA001077.

McCorkle, D. C., B. H. Corliss, and C. A. Farnham (1997), Vertical distributions and stable isotopic compositions of live (stained) benthic foraminifera from the North Carolina and California continental margins, *Deep Sea Res., Part I*, *44*(6), 983–1024, doi:10.1016/S0967-0637(97)00004-6.

McKenna, V. S., and W. L. Prell (2004), Calibration of the Mg/Ca of Globorotalia truncatulinoides (R) for the reconstruction of marine temperature gradients, *Paleoceanography*, *19*, PA2006, doi:10.1029/2000PA000604.

Mitchell, A., G. H. Brown, and R. Fuge (2001), Minor and trace element export from glacierized Alpine headwater catchment (Haut Glacier d'Arolla, Switzerland), *Hydrol. Process.*, *15*, 3499–3524, doi:10.1002/hyp.1041.

Montero-Serrano, J. C., V. Bout-Roumazeilles, N. Tribovillard, T. Sionneau, A. Riboulleau, A. Bory, and B. Flower (2009), Sedimentary evidence of deglacial megafloods in the northern Gulf of Mexico (Pigmy Basin), *Quat. Sci. Rev.*, *28*(27–28), 3333–3347, doi:10.1016/j.quascirev.2009.09.011.

Moore, W. S. (1999), The subterranean estuary: A reaction zone of ground water and sea water, *Mar. Chem.*, *65*, 111–125, doi:10.1016/S0304-4203(99)00014-6.

Moore, W. S., and T. J. Shaw (1998), Chemical signals from submarine fluid advection onto the continental shelf, *J. Geophys. Res.*, *103*, 21,543–21,552, doi:10.1029/98JC02232.

Murphy, S. J., H. E. Hurlburt, and J. J. O'Brien (1999), The connectivity of eddy variability in the Caribbean Sea, the Gulf of Mexico, and the Atlantic Ocean, *J. Geophys. Res.*, *104*, 1431–1453, doi:10.1029/1998JC900010.

Murton, J. B., M. D. Bateman, S. R. Dallimore, J. T. Teller, and Z. R. Yang (2010), Identification of Younger Dryas outburst flood path from Lake Agassiz to the Arctic Ocean, *Nature*, *464*(7289), 740–743, doi:10.1038/nature08954.

Nürnberg, D., J. Bijma, and C. Hemleben (1996), Assessing the reliability of magnesium in foraminiferal calcite as a proxy for water mass temperatures, *Geochim. Cosmochim. Acta*, *60*(5), 803–814, doi:10.1016/0016-7037(95)00446-7.

Nürnberg, D., M. Ziegler, C. Karas, R. Tiedemann, and M. W. Schmidt (2008), Interacting Loop Current variability and Mississippi River discharge over the past 400 kyr, *Earth Planet Sci. Lett.*, *272*(1–2), 278–289, doi:10.1016/j.epsl.2008.04.051.

Oppo, D. W., Y. Rosenthal, and B. K. Linsley (2009), 2,000-year-long temperature and hydrology reconstructions from the Indo-Pacific warm pool, *Nature*, *460*(7259), 1113–1116, doi:10.1038/nature08233.

Ortner, P. B., T. N. Lee, P. J. Milne, R. G. Zika, M. E. Clarke, G. P. Podesta, P. K. Swart, P. A. Tester, L. P. Atkinson, and W. R. Johnson (1995), Mississippi River flood waters that reached the Gulf Stream, *J. Geophys. Res.*, *100*, 13,595–13,601, doi:10.1029/95JC01039.

Otto-Bliesner, B. L., and E. C. Brady (2010), The sensitivity of the climate response to the magnitude and location of freshwater forcing: Last glacial maximum experiments, *Quat. Sci. Rev.*, *29*(1–2), 56–73.

Peterson, L. C., and G. H. Haug (2006), Variability in the mean latitude of the Atlantic Intertropical Convergence Zone as recorded by riverine input of sediments to the Cariaco Basin (Venezuela), *Palaeogeogr. Palaeoclimatol. Palaeoecol.*, *234*(1), 97–113, doi:10.1016/j.palaeo.2005.10.021.

Peterson, L. C., G. H. Haug, K. A. Hughen, and U. Rohl (2000), Rapid changes in the hydrologic cycle of the tropical Atlantic during the last glacial, *Science*, *290*, 1947–1951, doi:10.1126/science.290.5498.1947.

Rahmstorf, S. (2002), Ocean circulation and climate during the past 120,000 years, *Nature*, *419*(6903), 207–214, doi:10.1038/nature01090.

Rasmussen, S. O., et al. (2006), A new Greenland ice core chronology for the last glacial termination, *J. Geophys. Res.*, *111*, D06102, doi:10.1029/2005JD006079.

Rosenthal, Y., E. A. Boyle, and N. Slowey (1997), Temperature control on the incorporation of magnesium, strontium, fluorine, and cadmium into benthic foraminiferal shells from Little Bahama Bank: Prospects for thermocline paleoceanography, *Geochim. Cosmochim. Acta*, *61*(17), 3633–3643, doi:10.1016/S0016-7037(97)00181-6.

Rosenthal, Y., G. P. Lohmann, K. C. Lohmann, and R. M. Sherrell (2000), Incorporation and preservation of Mg in *Globigerinoides sacculifer* implications for reconstructing the temperature and ^{18}O/^{16}O of seawater, *Paleoceanography*, *15*(1), 135–145, doi:10.1029/1999PA000415.

Rühlemann, C., S. Mulitza, P. J. Muller, G. Wefer, and R. Zahn (1999), Warming of the tropical Atlantic ocean and slowdown of thermohaline circulation during the last deglaciation, *Nature*, *402*, 511–514, doi:10.1038/990069.

Russell, A. D., B. Honisch, H. J. Spero, and D. W. Lea (2004), Effects of seawater carbonate ion concentration and temperature on shell U, Mg, and Sr in cultured planktonic foraminifera, *Geochim. Cosmochim. Acta*, *68*(21), 4347–4361, doi:10.1016/j.gca.2004.03.013.

Schmidt, G. A., G. R. Bigg, and E. J. Rohling (1999), Global Seawater Oxygen-18 Database, http://data.giss.nasa.gov/o18data/, GSFC Earth Sci. (GES) DAAC, Greenbelt, Md.

Schmidt, M. W., H. J. Spero, and D. W. Lea (2004), Links between salinity variation in the Caribbean and North Atlantic thermohaline circulation, *Nature*, *428*, 160–163, doi:10.1038/nature02346.

Schmidt, M. W., M. J. Vautravers, and H. J. Spero (2006), Rapid subtropical North Atlantic salinity oscillations across Dansgaard-Oeschger cycles, *Nature*, *443*, 561–564, doi:10.1038/nature05121.

Schmidt, M. W., and H. J. Spero (2011), Meridional shifts in the marine ITCZ and the tropical hydrologic cycle over the last three glacial cycles, *Paleoceanography*, *26*, PA1206, doi:10.1029/2010PA001976.

Schmitz, W. J., and P. L. Richardson (1991), On the sources of the Florida Current, *Deep Sea Res., Part A*, *38*, 379–409.

Schrag, D. P. (1999), Rapid analysis of high-precision Sr/Ca ratios in corals and other marine carbonates, *Paleoceanography*, *14*(2), 97–102, doi:10.1029/1998PA900025.

Schrag, D. P., J. F. Adkins, K. McIntyre, J. L. Alexander, D. A. Hodell, C. D. Charles, and J. F. McManus (2002), The oxygen isotopic composition of seawater during the Last Glacial Maximum, *Quat. Sci. Rev.*, *21*, 331–342, doi:10.1016/S0277-3791(01)00110-X.

Siddall, M., T. F. Stocker, and P. U. Clark (2009), Constraints on future sea-level rise from past sea-level change (Retracted article. See vol. 3, pg. 217, 2010), *Nat. Geosci.*, *2*(8), 571–575, doi:10.1038/ngeo587.

Sionneau, T., V. Bout-Roumazeilles, B. P. Flower, A. Bory, N. Tribovillard, C. Kissel, B. Van Vliet-Lanoe, and J. C. M. Serrano (2010), Provenance of freshwater pulses in the Gulf of Mexico during the last deglaciation, *Quat. Res.*, *74*(2), 235–245, doi:10.1016/j.yqres.2010.07.002.

Spero, H. J., K. M. Mielke, E. M. Kalve, D. W. Lea, and D. K. Pak (2003), Multispecies approach to reconstructing eastern equatorial Pacific thermocline hydrography during the past 360 kyr, *Paleoceanography*, *18*(1), 1022, doi:10.1029/2002PA000814.

Stansell, N. D., M. B. Abbott, V. Rull, D. T. Rodbell, M. Bezada, and E. Montoya (2010), Abrupt Younger Dryas cooling in the northern tropics recorded in lake sediments from the Venezuelan Andes, *Earth Planet. Sci. Lett.*, *293*(1–2), 154–163, doi:10.1016/j.epsl.2010.02.040.

Stidd, C. K. (1967), The use of eigenvectors for climate estimates, *J. Appl. Meteorol.*, *6*, 255–264, doi:10.1175/1520-0450(1967)006<0255:TUOEFC>2.0.CO;2.

Stouffer, R. J., et al. (2006), Investigating the causes of the response of the thermohaline circulation to past and future climate changes, *J. Clim.*, *19*(8), 1365–1387, doi:10.1175/JCLI3689.1.

Sturges, W., and R. Leben (2000), Frequency of ring separations from the Loop Current in the Gulf of Mexico: A revised estimate, *J. Phys. Oceanogr.*, *30*, 1814–1819, doi:10.1175/1520-0485(2000)030<1814:FORSFT>2.0.CO;2.

Turekian, K. K., and D. G. Johnson (1966), The barium distribution in sea water, *Geochim. Cosmochim. Acta*, *30*, 1153–1174, doi:10.1016/0016-7037(66)90035-4.

Vellinga, M., and R. A. Wood (2002), Global climatic impacts of a collapse of the Atlantic thermohaline circulation, *Clim. Change*, *54*, 251–267, doi:10.1023/A:1016168827653.

Vellinga, M., and P. L. Wu (2004), Low-latitude freshwater influence on centennial variability of the Atlantic thermohaline circulation, *J. Clim.*, *17*(23), 4498–4511, doi:10.1175/3219.1.

Vukovich, F. M. (1988), Loop Current boundary variations, *J. Geophys. Res.*, *93*, 15,585–15,591, doi:10.1029/JC093iC12p15585.

Waelbroeck, C., et al. (2009), Constraints on the magnitude and patterns of ocean cooling at the Last Glacial Maximum, *Nat. Geosci.*, *2*(2), 127–132, doi:10.1038/ngeo411.

Waliser, D. E., and C. Gautier (1993), A satellite-derived climatology of the ITCZ, *J. Clim.*, *6*(11), 2162–2174, doi:10.1175/1520-0442(1993)006<2162:ASDCOT>2.0.CO;2.

Wan, X. Q., P. Chang, R. Saravanan, R. Zhang, and M. W. Schmidt (2009), On the interpretation of Caribbean paleo-temperature reconstructions during the Younger Dryas, *Geophys. Res. Lett.*, *36*, L02701, doi:10.1029/2008GL035805.

Wan, X. Q., P. Chang, and M. W. Schmidt (2010), Causes of tropical Atlantic paleo-salinity variation during periods of reduced AMOC, *Geophys. Res. Lett.*, *37*, L04603, doi:10.1029/2009GL042013.

Wang, Y. J., H. Cheng, R. L. Edwards, Z. S. An, J. Y. Wu, C. C. Shen, and J. A. Dorale (2001), A high-resolution absolute-dated Late Pleistocene monsoon record from Hulu Cave, China, *Science*, *294*(5550), 2345–2348, doi:10.1126/science.1064618.

Weldeab, S., R. R. Schneider, and M. Kolling (2006), Deglacial sea surface temperature and salinity increase in the western tropical Atlantic in synchrony with high latitude climate instabilities, *Earth Planet. Sci. Lett.*, *241*(3–4), 699–706, doi:10.1016/j.epsl.2005.11.012.

Weldeab, S., D. W. Lea, R. R. Schneider, and N. Andersen (2007), 155,000 years of West African monsoon and ocean thermal evolution, *Science*, *316*(5829), 1303–1307, doi:10.1126/science.1140461.

Williams, C., B. P. Flower, D. W. Hastings, A. M. Shiller, and E. A. Goddard (2010), A multi-proxy approach to deglacial paleo-salinity reconstructions based on Gulf of Mexico sediments, Abstract PP33B-1677 presented at 2010 Fall Meeting, AGU, San Francisco, Calif., 13–17 Dec.

Zaucker, F., and W. S. Broecker (1992), The influence of atmospheric moisture transport on the fresh water balance of the Atlantic drainage basin: General circulation model simulations and observations, *J. Geophys. Res.*, *97*, 2765–2773.

Zhang, R., and T. L. Delworth (2005), Simulated tropical response to a substantial weakening of the Atlantic thermohaline circulation, *J. Clim.*, *18*, 1853–1860, doi:10.1175/JCLI3460.1.

J. Lynch-Stieglitz, School of Earth and Atmospheric Sciences, Georgia Institute of Technology, Atlanta, GA 30307, USA.

M. W. Schmidt, Department of Oceanography, Texas A&M University, College Station, TX 77843, USA. (schmidt@ocean.tamu.edu)